Ground-state Fidelity in frustrated and unfrustrated models

Brtan, Daria

UNIVERSITY OF ZAGREB
FACULTY OF SCIENCE
DEPARTMENT OF PHYSICS

Daria Brtan

GROUND-STATE FIDELITY IN FRUSTRATED AND UNFRUSTRATED MODELS

Master Thesis

Zagreb, 2021

SVEUČILIŠTE U ZAGREBU
PRIRODOSLOVNO-MATEMATIČKI FAKULTET
FIZIČKI ODSJEK

Daria Brtan

VJERNOST OSNOVNOG STANJA U FRUSTRIRANIM I NEFRUSTRIRANIM KVANTNIM MODELIMA

Diplomski rad

Zagreb, 2021.

UNIVERSITY OF ZAGREB
FACULTY OF SCIENCE
DEPARTMENT OF PHYSICS

INTEGRATED UNDERGRADUATE AND GRADUATE UNIVERSITY
PROGRAMME IN PHYSICS

Daria Brtan

Master Thesis

Ground-state fidelity in frustrated and unfrustrated models

Advisor: Salvatore Marco Giampaolo, dr. sc.

Co-Advisor: assoc. prof. Davor Horvatić, dr. sc.

Master Thesis grade: _____

Committee: 1. _____

2. _____

3. _____

Master Thesis defence date: _____

Zagreb, 2021

I want to take this moment to thank my advisor dr. sc. Salvatore Marco Giampaolo, along with my unofficial co-advisor dr. sc. Fabio Franchini. Not only have they guided me professionally through this journey, but the support and understanding they offered helped me become more confident and realize my potential. Your help went above and beyond of "just" thesis advisory and for that, I am deeply grateful.

Additionally, I want to thank the whole group at the Institute, especially Alberto. You made me feel welcome and had time for all my questions, no matter how little. Also, you made this whole process easier, but more importantly, a lot more enjoyable.

I want to thank my family. My parents for recognizing and cultivating my pursuit of science throughout my life. Especially in my college education, their love, understanding, and unconditional support brought me to the finish line. My brother and sister have deeply motivated me with their advice and success since I was a little girl up to this day, and for that I am thankful. I thank my grandmother for worrying I get enough sleep, and my nieces and their laughter for making sure I do not.

Finally, I want to thank Matija, my biggest ally and motivator, whose help, reassurance, and encouragement were with me every step of the way. You believed in me even when I was unable to, and somehow, that was enough to keep me going, making all of this possible.

Željela bih zahvaliti mentoru dr. sc. Salvatoru Marcu Giampaolu, kao i neslužbenom ko-mentoru dr. sc. Fabiju Franchiniju. Vaše mentorstvo bilo je korak iznad pukog profesionalnog savjetovanja, te sam duboko zahvalna zbog podrške i poticaja koje ste mi pružili.

Nadalje htjela bih se zahvaliti cijeloj grupi sa Instituta, a posebice Albertu. Učinili ste da se osjećam dobrodošlo, imali strpljenja za sva moja pitanja te učinili cijeli ovaj proces puno ugodnijim.

Zahvalna sam na svojoj obitelji. Hvala mojim roditeljima koji su prvo prepoznali, a zatim i poticali moju ljubav prema znanosti cijeli moj život, a posebice tijekom studiranja. Vaša ljubav, razumijevanje i bezuvjetna potpora doveli su me do cilja. Uspjesi i savjeti mog brata i sestre motiviraju me odmalena i na tomu sam im izrazito zahvalna. Hvala mojoj baki koja se uvijek brinula da ne spavam dovoljno, i mojim nećakinjama čiji se jutarnji smijeh pobrinuo za to.

Za kraj, želim zahvatili Matiji, mom najvećem savezniku, koji me podržavao, ohrabrivao i pomagao mi čitavim putem. Vjerovao si u mene i kada je meni samoj to bilo teško, što mi je često bila dovoljna motivacija da nastavim.

Vjernost osnovnog stanja u frustriranim i nefrustriranim kvantnim modelima

Sažetak

Sustav koji ima *frustrirane rubne uvjete*, tj. neparan broj spinova spojenih u prsten ili periodičke rubne uvjete, uz antiferomagnetično uređenje, nazivamo frustriranim. Posljednjih godina pokazano je da rubni uvjeti mogu utjecati na svojstva sustava.

U ovom radu određuju se svojstva geometrije osnovnog stanja XY lanca računanjem vjernosti (engl. *fidelity*) i pripadajuće susceptibilnosti kako bi se usporedili frustrirani i nefrustrirani sustav te na taj način proučio utjecaj frustracije na spomenuta svojstva i veličine sustava. Kao sustav izabran je 1D XY model jer je egzaktno rješiv. Korištena je vjernost budući da mjeri udaljenost tj. sličnost dvaju stanja, te bi kao takva, pri nailasku na kritičnu točku tijekom variranja parametara hamiltonijana, trebala imati (gotovo) diskontinuirani pad. Nadalje, računajući susceptibilnost vjernosti u regijama gdje ga je moguće definirati, određen je kvantni metrički tenzor koji opisuje geometriju osnovnog stanja sustava.

Najprije je riješen XY model te je klasificirano njegovo osnovno stanje ovisno o parametru vezanja J, paritetu broja spinova i sektora te s obzirom na poziciju u parametarskom prostoru. Posebno pomno praćeno je osebujno ponašanje uzrokovano frustracijama. Nakon toga, izračunata je vjernost svih osnovnih stanja te diskutiran rezultat u ovisnosti o regiji parametarskog prostora kojoj sustav pripada. Vjernost je pokazala padove na očekivanim kritičnim linijama h=1,γ =0, no također i mnoštvo egzaktnih diskontinuiteta u frustriranoj regiji parametarskog prostora. Spomenuti diskontinuiteti potječu od promjene energetskih nivoa uzrokovanih promjenom ekscitacije u osnovnom stanju koje ovisi o parametrima h i γ. Kako je vjernost identički nula, susceptibilnosti vjernosti ne može se niti definirati u frustriranoj regiji. Stoga je uvedena nova mjera, reducirana vjernost kako bi se "omekšala" ortogonalnost i omogućio izračun susceptibilnosti. Pomoću navedene mjere pokazano je da navedeni pomaci energetskih nivoa nestaju u termodinamičkom limesu te nisu znak faznog prijelaza, što je prvi, nama poznat, protuprimjer široko priznatoj pretpostavci da se vjernost može koristiti za karakterizaciju sustava bez *a priori* znanja o sustavu.

Ključne riječi: frustracija, vjernost, susceptibilnost vjernosti, 1D XY model

Ground-state fidelity in frustrated and unfrustrated models

Abstract

A system with *frustrated boundary conditions*, which consist of an odd number of spins enclosed in a antiferromagnetic ring (or have periodic boundary conditions), is frustrated. In recent years it has been shown that boundary conditions can affect the system's characteristics.

In this work, we compute the properties of the ground state geometry for the XY chain by means of calculating the fidelity and its susceptibility to compare the unfrustrated and frustrated models and observe the effects of frustration on it. The 1D XY model is chosen for its exact analytical solution. Fidelity is used because, as a measure of the states overlap, it is supposed to show (almost) discontinuous drops upon reaching critical points in slow variation of the parameters of the Hamiltonian. Moreover, the quantum metric tensor, describing the ground state manifold of the system, can be constructed by calculating fidelity susceptibility.

We start by comprehensively solving the XY chain and classifying its ground states according to J coupling, the parity of the number of spins and different regions of the parameter space. Special care was taken of the peculiar behaviour due to frustration.

Next, we compute the overlaps for all ground states and discuss the results based on regions. The fidelity drops at the expected critical lines $h = 1$ and $\gamma = 0$, but also shows exact discontinuity in the frustrated region $h < 1 - \gamma^2$. These correspond to level-crossings generated by change of excitation in the ground state which is dependant on the parameters h and γ. This hindered efforts to calculate the associated susceptibility, so a new measure was used reduced fidelity to "soften" the orthogonality and facilitate the calculation of susceptibility. We discover these level-crossings vanish in the thermodynamic limit and do not constitute phase transitions, which is, to our knowledge, the first counter example to the widely-accepted assumption that the fidelity approach can be used to characterise systems without any *a priori* knowledge of the system.

Keywords: frustration, fidelity, fidelity susceptibility, 1D XY model

Contents

1 Introduction

"The whole is greater than the sum of its parts." A (sort of) misquoted Aristotle's saying is often used to express the emergent nature of many-body systems. Namely, when a (large) collection of items exhibits some phenomena or property which is not present at the level of each constituent, that system has displayed emergence. Whereas complex systems surrounding us in basically every aspect of human life can have other manifestations of complexity (such as chaotic behavior associated with, among others, severe sensitivity to initial conditions), the term *many-body system* is generally pertaining to the physical category of large systems consisting of many particles with, predominately quantum, interactions. *Many* is then understood as anything larger than the number two, although systems of three and four "bodies" are customarily separated and referred to as "few-body problems" because they can still be treated using some specific methods. Although, in principle, one could describe a system with an effectively infinite number of components by writing the Schrödinger's equation, including all its interactions, the solution of that system of equations is, for all intents and purposes, impossible. Thus, solving these problems chiefly entails creating models which capture the relevant interactions (relying on a great number of approximations), as opposed to the reductionist approach of explaining systems through their parts. In physics, emergence implies the existence of traits at macroscopic and their non-existence at microscopic scales. This is in contrast with the often-used approach of studying a macroscopic system through an ensemble of microscopic systems.

A star of the reductionist approach is the Landau-Ginzburg theory. With its concept of a local order parameter being the main characterization of a phase transition, it perfectly embodies the endeavor of encompassing as many situations as possible under a single umbrella of a framework containing as few variables as possible. This order parameter grows from zero to a finite value by crossing over a point/line (in parameter space) which is then called critical. If it grows continuously, the transition is deemed second order, where if it does so with a discontinuity it is a first order transition. The key idea of the theory rests on symmetries of the system, as the order parameter is associated with a breaking of a specific symmetry. Other aspects, such as the boundary conditions, are not relevant for the forming of a specific order.

Since the 1950s the Landau formulation has been used to classify classical many-body systems [1]. Moving onto quantum systems, the theory has been reapplied without much adjustment [2]. However, soon thereafter it became clear it was not well suited for the decidedly richer landscape of quantum complex systems [3]. For instance, recently, the notion that boundary conditions are negligible has been challenged. It was observed that a specific set of boundary conditions can induce a phenomenon termed frustration which affects and modifies various system characteristics, e.g. the energy gap, or even destroy the order parameter [4–7]. While frustration is a broad concept, fundamentally, it stems from the impossibility to satisfy all constraints of the system at the same time. Moreover, although most quantum Hamiltonians consist of terms which impose competing orders, geometrical frustration is the one usually referred to. Its essence can be understood through a fairly simple “model”. First, picture an antiferromagnetic, square "chain" with four spins in its vertices. To satisfy antiferromagnetic conditions, all one needs to do is alternately put spins up or down, as shown on Figure 1.1a). In another setting, for example a triangle, when the same is tried, one finds it is impossible. We say the system is frustrated as it cannot meet its boundary conditions, which consist of an odd number of spins enclosed in a antiferromagnetic ring. This type of boundary conditions are named *frustrated boundary conditions* or FBC. The ring structure can also be exchanged for periodic boundary conditions.

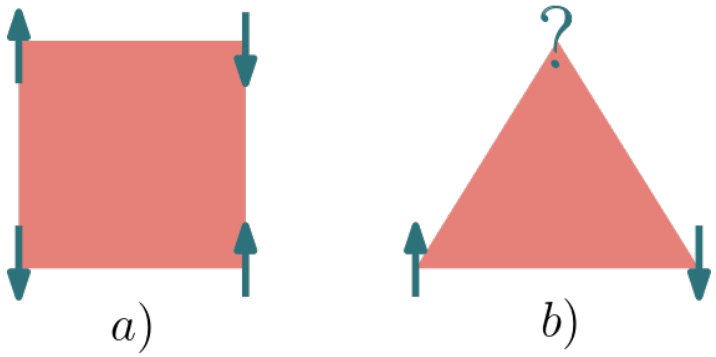

Figure 1.1: A schematic depiction of frustration in a closed "chain" system. In a) we can see a normal antiferromagnetic system, where in b) the system cannot meet its boundary conditions and is therefore frustrated.

The main goal of this work will be to study the geometrical effects of frustration through comparison with the unfrustrated situation. In other words, we will examine the ground state manifold induced by the quantum metric tensor. The quantum

metric tensor is the real, symmetric part of a complex quantum geometric tensor, and it fulfills the role of measuring the distance (i.e. the overlap) between two states, i.e., the role of a metric. Using the metric tensor, we can visualize the ground state manifold and build an equivalent surface [8, 9]. This analysis will be based on the XY chain in a transverse magnetic field.

The one-dimensional XY model in a transverse magnetic field is chosen for a variety of reasons. As a generalization of the Ising model, it is a prototypical quantum mechanical model for magnetic-orderings in spin systems. Along with the Ising model next-neighbour xx interaction and an external magnetic field, it includes an interaction in the y components which differs from the x interaction in a way described by the anisotropy parameter γ. The Hamiltonian is given by

$$H = \frac{J}{2}\sum_{j=1}^{N}\left(\frac{1+\gamma}{2}\sigma_j^x\sigma_{j+1}^x + \frac{1-\gamma}{2}\sigma_j^y\sigma_{j+1}^y\right) - \frac{h}{2}\sum_{j=1}^{N}\sigma_j^z, \tag{1.1}$$

and it describes a 1D lattice with N sites, and on each site there is a three-dimensional $1/2$ spin given by Pauli matrices. For $\gamma = 0$ the system reduces to an isotropic XX model, where for $\gamma = \pm 1$, one gets the 1D quantum Ising model. As for the coupling J, in this definition the $J < 0$ corresponds to the ferromagnetic ordering whereas the $J > 0$ case would describe antiferromagnetic order. We take these parameters to be dimensionless from now on. To check this it is enough to reduce the system to the Ising scenario by setting $\gamma = 1, \quad h = 0$ where it is easy to see that $J < 0$ brings a parallel alignment of spins while $J > 0$ creates antiparallel neighbouring spins. Furthermore, in order to study frustration, we will assume periodic boundary conditions, i.e., a closed chain. Finally, we will work in the first quadrant of the parameter space $\gamma \geq 0, \quad h \geq 0$ as the symmetries of the model guarantee allow access to the rest of the parameter space. Strictly speaking, a $\gamma \to -\gamma$ transformation is achieved by a rotation $\pi/2$ around the z-axis and corresponds to a switch between x and y interaction. On the other hand, by mirroring the z-axis to change its direction and then rotating by $\pi/2$ around it $h < 0$ can be reached. The XY chain Hamiltonian also commutes with the parity operator $P = \prod_{l=1}^{N}\sigma_l^z$, which implies that it possesses a $\mathcal{Z}_2$ symmetry.

One of the biggest advantages of this model is that it is exactly solvable, which makes it ideal for testing out new methods. Essentially any quantity, from the ground

state and its excitations, to the free energy and entanglement entropy, can be found analytically and exactly. Despite having an analytical solution, it is not overly simple but it has a rich (quantum) phase diagram at absolute zero $T = 0$ consisting of two phase transitions. Quantum phase transitions (QPTs), unlike classical phase transitions which are caused by thermal fluctuations, are caused by quantum fluctuations at absolute zero temperature. The quantum fluctuations involve (drastic) changes in the ground state properties of a system, induced by variation of the system's driving parameters, i.e. the interactions between the system's components. As already mentioned, QPTs are also treated by the classical Landau-Ginsburg approach, albeit with some caveats. For example, quantum phase transitions have created the need for expanding on the premise of order parameters from local to not-so-local and even global parameters in order to preserve the idea that a critical point must separate two phases with different macroscopic behaviours.

The XY chain has two critical lines in its quantum phase diagram, one corresponding to the Ising transition at $h = 1$ and the other $\gamma = 0$, matching the so-called XX model. The $h = 1$ transition is associated with the $\mathcal{Z}_2$ symmetry breaking, as the system crosses from a non-degenerate state in $h > 1$ into a degenerate state for $h < 1$ in the thermodynamic limit, while crossing the $\gamma = 0$ transition switches the roles of x and y.

When frustration is brought into the mix, another interesting region emerges. For the ground state of the system in region $h < 1 - \gamma^2$, the system favors a particular excited state over the expected vacuum, as a result of frustration. These excitations will then induce a series of level-crossings which, despite (technically) persevering in the thermodynamic limit, do not constitute a phase transition.

To investigate how frustration affects the geometrical properties of the ground state, we will not use the standard technique, but a novel approach which has been put forward in recent years. As more and more quantum information measures have proved useful in other areas of physics, fidelity and its susceptibility has been introduced as a new approach to phase transition analysis [10–16]. Fidelity is basically an overlap function, and as such, it is a measure of the closeness between two states.

$$F(\Psi', \Psi) = |\langle \Psi' | \Psi \rangle|, \tag{1.2}$$

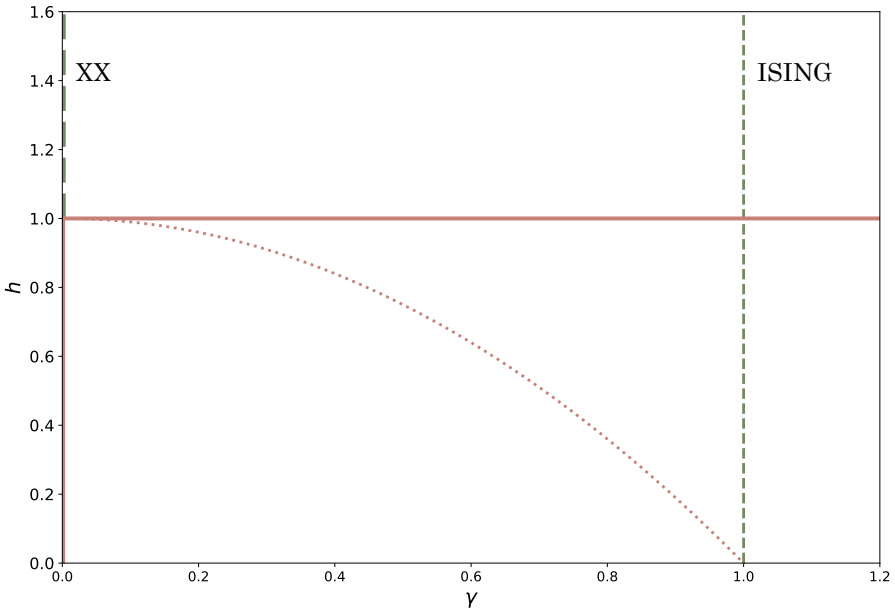

Figure 1.2: Phase diagram at T=0 for the 1D XY chain. The $\gamma = 0$ line matches the XX model, and it is critical for $h \leq 1$. The $\gamma = 1$ line corresponds to the Ising model and it intersects the critical $h = 1$ line.

where $|\Psi\rangle$ and $|\Psi'\rangle$ are two normalized states. If two states are identical, it produces unity, while for two orthogonal states it gives zero. Since QPTs are directly evidenced by a sudden change in the ground state, the potential usefulness of fidelity can be promptly recognized. Suppose a parametric Hamiltonian $H(\vec{\lambda})$ had a QPT at a critical point $\vec{\lambda}_c$. If one were to move through the parameter space with some change $d\vec{\lambda}$ and map the fidelity between each two ground states associated with two points differing by $d\vec{\lambda}$, they would see a clear signature of that transition. In most of the parameter space, the overlap between two points is as close to 1 as the step allows. However, at (and slightly around it) $\vec{\lambda}_c$ the ground state changes dramatically between two points and consequently the overlap will have a drop. That drop will become sharper and deeper as the system size is increased, turning into a divergence in the thermodynamic limit. By furthering the analysis and looking at the fidelity susceptibility, in addition to critical points the critical exponents can be extracted [15]. Moreover, it has been shown that from the susceptibility it is possible to construct a metric tensor in parameter space, whose components become singular at quantum critical points [9], which is one of the reasons why this particular method has been chosen.

However, in systems encountering a series of level-crossings systems a different approach is required. One such approach is reduced fidelity, an overlap between subsystems which then reduces the degree of orthogonality and allows for further inspection. [17, 18] It is defined as a fidelity between two reduced density matrices instead of full density operators. Fidelity can also be written in a more general way as

$$\mathcal{F}(\rho,\sigma) \coloneqq \text{tr}\left(\sqrt{\rho^{1/2}\sigma\rho^{1/2}}\right). \tag{1.3}$$

By tracing out a part of the system, we obtain a formula for the reduced fidelity.

$$\mathcal{F}^R = \text{Tr}\,\sqrt{\rho^{1/2}\tilde{\rho}\rho^{1/2}}. \tag{1.4}$$

Up to now, it has been widely presumed that the real advantage of the fidelity approach is that it does not require any *a priori* knowledge about the system, such as the order parameter or symmetries, except its ground state geometry. In this work, by analysing the changes in the geometry of the XY chain ground state induced by frustration, we have encountered exact discontinuities in the fidelity which, through further analysis, have been proven not to be phase transitions, effectively acting as a counter example to the aforementioned presumption and potentially ridding the method of fidelity and its derivatives of its most promising feature.

We start by thoroughly solving the XY chain through standard procedure, and classifying its ground states according to J ordering, the parity of the number of spins and different regions of the parameter space in Section 2. In the next Section 3 we calculate the overlaps for relevant ground states and discuss the results based on regions in 3.1. We also derive and examine the associated susceptibility. Next, we calculate the correlation functions of the model in order to study the reduced fidelity and its susceptibility in 3.2.

2 Solving the quantum XY model

The XY chain was introduced as an exactly solvable model similar to the Heisenberg model by Lieb, Schultz and Mattis in 1961 [19], where it was solved in the absence of a magnetic field. Works including a finite magnetic field apperead soon after [20,21]. The problem is solved by mapping the chain to a system of free fermions. The XY Hamiltonian with anisotropy γ in a transverse magnetic field of strength h reads

$$H = \frac{J}{2}\sum_{j=1}^{N}\left(\frac{1+\gamma}{2}\sigma_j^x\sigma_{j+1}^x + \frac{1-\gamma}{2}\sigma_j^y\sigma_{j+1}^y\right) - \frac{h}{2}\sum_{j=1}^{N}\sigma_j^z. \tag{2.1}$$

It is expressed in terms of Pauli spin operators

$$\sigma_x = \begin{pmatrix} 0 & 1 \\ 1 & 0 \end{pmatrix}, \quad \sigma_y = \begin{pmatrix} 0 & -i \\ i & 0 \end{pmatrix}, \quad \sigma_z = \begin{pmatrix} 1 & 0 \\ 0 & -1 \end{pmatrix}. \tag{2.2}$$

In a system described by this Hamiltonian, there is a 1D lattice with N sites, and on each site there is a three-dimensional $1/2$ spin. In the presence of a magnetic field, the interaction between neighbours in the direction of the external magnetic field can be neglected. In (2.1), that direction is z. For $\gamma = 0$ the system reduces to a isotropic XX model, where for $\gamma = \pm 1$, one gets the 1D quantum Ising model. Also, it is important to emphasise that we have assumed periodic boundary conditions $\sigma_{N+1}^{\alpha} = \sigma_1^{\alpha}$.

This section will go over the well-established solution procedure consisting of a Jordan Wigner mapping from spins to fermions, tranforming those into Fourier space and rotating through a Bogoliubov transformation (Subsection 2.1) to finally obtain the diagonal Hamiltonian. Then, Subsection 2.2 will go into a detailed analysis of the ground state and the corresponding energies across different regions of the parameter space.

2.1 Solution procedure

2.1.1 Jordan Wigner transformation

Spins, even the simplest $1/2$'s, make mathematical manipulation hard since they are nor bosons nor fermions. That is why the Jordan-Wigner transformation is a powerful tool which enables us to map a system of, in this situation spins, to an equivalent

system of fermions, thereby immediately allowing an easier study and transfer of known properties to an unknown problem. By transforming N spins to N fermions, we get a Hamiltonian that can be further simplified, in the end giving us a clean diagonal quadratic fermion Hamiltonian whose ground state and energy are easily acquired, unlike our starting Hamiltonian.

It is convenient to write Hamiltonian (2.1) using Pauli raising and lowering operators ((2.2) for explicit definition of Pauli matrices used)

$$\sigma^{+,-} = \frac{1}{2}(\sigma^x \pm i\sigma^y). \tag{2.3}$$

Then, (2.1) reads (h.c. stands for the hermitian conjugate of the expression in brackets)

$$H = \frac{J}{2}\sum_{j=1}^{N}\left(\sigma_j^+\sigma_{j+1}^- + \gamma\sigma_j^+\sigma_{j+1}^+ + \text{h.c.}\right) - \sum_{j=1}^{N} h\sigma_j^z. \tag{2.4}$$

Reviewing the known properties of Pauli spin operators, we can see they are not Fermi operators

$$[\sigma_j^\alpha,\sigma_j^\beta] = 2i\epsilon_{\alpha\beta\gamma}\,\sigma_j^\gamma, \tag{2.5a}$$

$$[\sigma_i^\alpha,\sigma_j^\beta] = 0 \quad \text{for} \quad i \neq j. \tag{2.5b}$$

$$\{\sigma_j^\alpha,\sigma_j^\beta\} = 2\delta_{\alpha\beta}, \tag{2.5c}$$

Latin letters i, j stand for particular sites, while Greek letters α, β, γ stand for x, y or z. $\epsilon_{\alpha\beta\gamma}$ is the Levi-Civita symbol and $\delta_{\alpha\beta}$ the Kronecker delta. As these relations show, Pauli spins satisfy fermionic anti-commutation relations only on a particular site (2.5c), while between different sites they act bosonically. Furthermore, it can be shown (using (2.3) and (2.6)) that the set of operators σ_j^-, σ_j^+ and σ_j^z is also not a set of Fermi operators.

$$[\sigma_i^+,\sigma_j^-] = \delta_{i,j}\sigma_j^z, \tag{2.6a}$$

$$[\sigma_i^z,\sigma_j^+] = \delta_{i,j}\sigma_j^+, \tag{2.6b}$$

$$\{\sigma_j^+,\sigma_j^-\} = 1, \tag{2.6c}$$

$$\{\sigma_j^z,\sigma_j^+\} = 0. \tag{2.6d}$$

That is why we introduce the Jordan-Wigner transformation for the XY model; the Fermi annihilation and creation operators are, respectively

$$\psi_j = \left(\prod_{l=1}^{j-1} \sigma_l^z\right) \sigma_j^+, \tag{2.7a}$$

$$\psi_j^\dagger = \left(\prod_{l=1}^{j-1} \sigma_l^z\right) \sigma_j^-, \tag{2.7b}$$

for $j = 1, 2, ..N$. The product $\prod$ is used in place of tensor product symbol $\bigotimes$ for simplicity. Using the definition of these Fermi operators and properties of Pauli operators, it can be shown that ψ_j and $\psi_j^\dagger$ are Fermi operators

$$\{\psi_i, \psi_j\} = 0, \tag{2.8a}$$

$$\{\psi_i, \psi_j^\dagger\} = \delta_{ij}. \tag{2.8b}$$

This system's Hilbert space is a tensor product of N spin $1/2$ Hilbert spaces, and its basis are product spin states $|n_1\rangle \otimes |n_2\rangle \otimes ... |n_N\rangle$ or shortly $|n_1\, n_2 ... n_N\rangle$. The n_i stands for $\uparrow$ or $\downarrow$. If we identify $\uparrow$ with 0 and $\downarrow$ with 1, and use $\sigma^z\ |\uparrow\rangle = |\uparrow\rangle$ and $\sigma^z\ |\downarrow\rangle = -\,|\downarrow\rangle$, it follows

$$\psi_j\, |n_1 \dots n_j = 0 \dots n_N\rangle = 0, \tag{2.9a}$$

$$\psi_j\, |n_1 \dots n_j = 1 \dots n_N\rangle = (-1)^{n_1}(-1)^{n_2} \dots (-1)^{n_{j-1}}\, |n_1 n_2 \dots n_j = 0 \dots n_N\rangle\,, \tag{2.9b}$$

$$\psi_j^\dagger\, |n_1 \dots n_j = 0 \dots n_N\rangle = (-1)^{n_1}(-1)^{n_2} \dots (-1)^{n_{j-1}}\, |n_1 \dots n_j = 1 \dots n_N\rangle\,, \tag{2.9c}$$

$$\psi_j^\dagger\, |n_1 \dots n_j = 1 \dots n_N\rangle = 0, \tag{2.9d}$$

and finally,

$$\psi_j^\dagger \psi_j\, |n_1 ... n_j ... n_N\rangle = n_j\ |n_1 ... n_j ... n_N\rangle\,. \tag{2.9e}$$

As it naturally stems from (2.7), spin downs $\downarrow$ correspond to particles and spin ups $\uparrow$ to holes. It is convenient to define also the inverse relations for Pauli operators in terms of Fermi operators for $j = 1, .., N$

$$\sigma_j^z = 1 - 2\psi_j^\dagger \psi_j, \tag{2.10a}$$

$$\sigma_j^+ = \left(\prod_{l=1}^{j-1} 1 - 2\psi_l^\dagger \psi_l \right) \psi_j, \tag{2.10b}$$

$$\sigma_j^- = \left(\prod_{l=1}^{j-1} 1 - 2\psi_l^\dagger \psi_l \right) \psi_j^\dagger. \tag{2.10c}$$

Applying (2.10) to (2.4) we obtain

$$\begin{aligned} H = &- \frac{J}{2} \sum_{j=1}^{N-1} \left(\psi_j \psi_{j+1}^\dagger + \gamma \psi_j \psi_{j+1} + \text{ h.c. } \right) + \frac{J}{2} P \left(\psi_N \psi_1^\dagger + \gamma \psi_N \psi_1 + \text{ h.c. } \right) \\ &+ h \sum_{j=1}^{N} \psi_j^\dagger \psi_j - \frac{1}{2} N h. \end{aligned} \tag{2.11}$$

We isolated the $j = N$ case because defining a ψ_{N+1} operator would tamper with the Fermi commutation relations. We also introduced the Hermitian parity operator

$$P = \prod_{l=1}^{N} \sigma_l^z = \prod_{l=1}^{N} \left(1 - 2\psi_l^\dagger \psi_l \right). \tag{2.12}$$

The parity operator simply gives a plus (minus) sign on a state with even (odd) number of particles. Since the Hamiltonian (2.11) only has terms quadratic in Fermi operators (they come in pairs such as $\psi_i \psi_j$), the number of particles also only changes in pairs. Therefore, the Hamiltonian commutes with the parity operator $[H, P] = 0$. We see that (2.11) is not quadratic in Fermi operators, but if we separate our problem into two sectors based on parity P, we will have a quadratic form Hamiltonian in each sector, bringing us closer to the final diagonal form. We can do this by writing the Hamiltonian (2.11) as follows

$$H = \frac{1+P}{2} H^+ \frac{1+P}{2} + \frac{1-P}{2} H^- \frac{1-P}{2}. \tag{2.13}$$

Explicitly, H^+ and H^- are equal to (2.11), substituting P with ± 1

$$\begin{aligned} H^{\pm} = &- \frac{J}{2}\sum_{j=1}^{N-1}\left(\psi_j\psi_{j+1}^{\dagger} + \gamma\psi_j\psi_{j+1} + \text{ h.c. }\right) \pm \frac{J}{2}\left(\psi_N\psi_1^{\dagger} + \gamma\psi_N\psi_1 + \text{ h.c. }\right) \\ &+ h\sum_{j=1}^{N}\psi_j^{\dagger}\psi_j - \frac{1}{2}Nh, \end{aligned} \tag{2.14}$$

Also, now there is a convenient way to define ψ_{N+1} that will allow us to write (2.14) in a more concise way

$$\psi_{N+1}\left|P=1\right\rangle = -\psi_1\left|P=1\right\rangle, \tag{2.15a}$$

$$\psi_{N+1}\left|P=-1\right\rangle = \psi_1\left|P=-1\right\rangle, \tag{2.15b}$$

brings us

$$H^{\pm} = -\frac{J}{2}\sum_{j=1}^{N}(\psi_j\psi_{j+1}^{\dagger} + \gamma\psi_j\psi_{j+1} + \text{h.c.}) + h\sum_{j=1}^{N}\psi_j^{\dagger}\psi_j - \frac{1}{2}Nh. \tag{2.16}$$

2.1.2 Fourier transform of Fermi operators

We can define new operators ψ_q that play a role of a Fourier transform (for confirmation and informal proof see Appendix A.1)

$$\psi_q \equiv \frac{1}{\sqrt{N}}\sum_{l=1}^{N}\psi_l e^{-i\frac{2\pi}{N}ql}, \tag{2.17}$$

for any $q \in X_N$, with $X_N = \{x_0, x_0+1, x_0+2, ..., x_0+N-1\}$ and $x_0 = 1/2$ in the even sector and $x_0 = 0$ in the odd sector. These operators are periodic with period N $\psi_q = \psi_{q+N}$ so we can technically talk about all $q \in X_N + \mathbb{Z}$. It can be shown using (2.17), (2.8) and (A.1) that ψ_q are also Fermi operators

$$\{\psi_q, \psi_{q'}\} = 0 \tag{2.18a}$$

$$\{\psi_q, \psi_{q'}^{\dagger}\} = \delta_{qq'} \tag{2.18b}$$

Now, using (2.17), (2.18) and (A.1) we obtain the following

$$\sum_{j=1}^{N} \psi_j^\dagger \psi_{j+1} = \sum_q \psi_q^\dagger \psi_q e^{i\frac{2\pi}{N}q}, \tag{2.19a}$$

$$\sum_{j=1}^{N} \psi_j^\dagger \psi_{j+1}^\dagger = \sum_q \psi_q^\dagger \psi_{-q}^\dagger e^{i\frac{2\pi}{N}q} = i\sum_q \sin\left(\frac{2\pi}{N}q\right) \psi_q^\dagger \psi_{-q}^\dagger, \tag{2.19b}$$

$$\sum_{j=1}^{N} \psi_j^\dagger \psi_j = \sum_q \psi_q^\dagger \psi_q, \tag{2.19c}$$

Furthermore, we will redefine ψ_q by adding a phase factor (not harmful to Fermi relations (2.18)) to get rid of the imaginary unit

$$\psi_q \equiv \frac{e^{i\pi/4}}{\sqrt{N}} \sum_{l=1}^{N} \psi_l e^{-i\frac{2\pi}{N}ql}. \tag{2.20}$$

We now have Hamiltonians (2.16) in a form that is simpler to diagonalize

$$H^\pm = \sum_q \left[J\cos\left(\frac{2\pi}{N}q\right) + h\right]\left(\psi_q^\dagger \psi_q - \frac{1}{2}\right) + \frac{1}{2}J\gamma \sum_q \sin\left(\frac{2\pi}{N}q\right)\left(\psi_q^\dagger \psi_{-q}^\dagger + \psi_{-q}\psi_q\right). \tag{2.21}$$

An extra term $-\frac{J}{2}\sum_q \cos\frac{2\pi}{N}q = 0$ was added for aesthetic reasons.

2.1.3 Bogoliubov transformation

Bogoliubov transformation is a transformation that can be thought of as essentially a rotation of phase space which allows us to change Hamiltonian basis to one in which the Hamiltonian is diagonal. In the process, it will give us new creation and annihilation operators which will tell us the structure of the elementary excitations in our system. It will be the final step that will bring us to the free fermionic Hamiltonian in diagonal form.

The last formulation of Hamiltonians (2.21) can now be written in simple matrix notation

$$H^\pm = \frac{1}{2}\sum_q \begin{pmatrix} \psi_q^\dagger & \psi_{-q} \end{pmatrix} M_q \begin{pmatrix} \psi_q \\ \psi_{-q}^\dagger \end{pmatrix}, \tag{2.22}$$

where M_q are 2×2 symmetric matrices

$$M_q = \begin{pmatrix} h + J\cos\left(\frac{2\pi}{N}q\right) & -\gamma\sin\left(\frac{2\pi}{N}q\right) \\ -\gamma\sin\left(\frac{2\pi}{N}q\right) & -\left[h + J\cos\left(\frac{2\pi}{N}q\right)\right] \end{pmatrix} = \begin{pmatrix} a_q & b_q \\ b_q & -a_q \end{pmatrix}, \tag{2.23}$$

with coefficients:

$$a_q \equiv h + \cos\left(\frac{2\pi}{N}q\right), \tag{2.24a}$$

$$b_q \equiv -\gamma\sin\left(\frac{2\pi}{N}q\right). \tag{2.24b}$$

It is obvious that the matrix M_q is diagonal for $q = 0$ in the odd sector, while for $q = N/2$ it depends on the parity of N. It is convenient to also define

$$k = \frac{2\pi}{N}q.$$

With this definition it is easy to see why $q = N/2$ can, and will be referred to as the π-mode. Further in this work we will use q or k solely based on convenience. The matrices M_k for the 0 and π mode are

$$M_{k=0} = \begin{pmatrix} h + J & 0 \\ 0 & -(h + J) \end{pmatrix}, \quad M_{k=\pi} = \begin{pmatrix} h - J & 0 \\ 0 & -(h - J) \end{pmatrix}. \tag{2.25}$$

Now, let us examine the case(s) when $k \neq 0, \pi$. In this case(s) the matrix M_q is not diagonal but it is symmetric so it can be diagonalized by an orthogonal matrix O_q

$$M_q = O_q^T D_q O_q, \tag{2.26}$$

with D_q being a diagonal matrix. We can define O_q as a rotation matrix

$$O_q = \begin{pmatrix} \cos\theta_q & -\sin\theta_q \\ \sin\theta_q & \cos\theta_q \end{pmatrix}, \tag{2.27}$$

which allows us to write

$$O_q \begin{pmatrix} \psi_q \\ \psi_{-q}^\dagger \end{pmatrix} = \begin{pmatrix} \cos\theta_q\psi_q - \sin\theta_q\psi_{-q}^\dagger \\ \sin\theta_q\psi_q + \cos\theta_q\psi_{-q}^\dagger \end{pmatrix}. \tag{2.28}$$

Since the columns of O_q^T are the eigenvectors of M_q, we get the expressions for $\cos\theta_q$ and $\sin\theta_q$ by solving the eigenvalue problem for the matrix M_q (2.23). By this procedure we will also get the diagonal matrix D_q. Here are the results

$$\cos\theta_q = \frac{b_q}{\sqrt{2}\sqrt{a_q^2+b_q^2-a_q\sqrt{a_q^2+b_q^2}}}, \tag{2.29a}$$

$$\sin\theta_q = \frac{a_q-\sqrt{a_q^2+b_q^2}}{\sqrt{2}\sqrt{a_q^2+b_q^2-a_q\sqrt{a_q^2+b_q^2}}}, \tag{2.29b}$$

and

$$D_q = \begin{pmatrix} \Lambda_q & 0 \\ 0 & -\Lambda_q \end{pmatrix} \tag{2.30}$$

with Λ_q:

$$\Lambda_q \equiv \Lambda\left(\frac{2\pi}{N}q\right) \equiv \sqrt{\left[h+J\cos\left(\frac{2\pi}{N}q\right)\right]^2 + J^2\gamma^2\sin^2\left(\frac{2\pi}{N}q\right)}. \tag{2.31}$$

It is convenient to define the function Λ_k to incorporate the special modes $k=0,\pi$.

$$\Lambda_{k=0} = |h+J|, \tag{2.32a}$$

$$\Lambda_{k=\pi} = |h-J|. \tag{2.32b}$$

This is an important addition to the energy function Λ_q. It turns out that, although the function obtained by diagonalization is strictly positive, for specific momenta $k=0,\pi$, diagonalization is avoided and by that the obligatory positivity. In these special momenta it is possible to have negative energy, depending on the value of h and both the magnitude of J and its sign. The gravity of this fact and its consequence will be discussed further in the next subsection.
Now, looking at (2.28) and considering the property

$$\cos\theta_{-q} = -\cos\theta_q, \quad \sin\theta_{-q} = \sin\theta_q, \tag{2.33}$$

(which comes out of (2.29)) we can see it is convenient to define operators

$$\chi_q \equiv \cos\theta_q\psi_q - \sin\theta_q\psi_{-q}^\dagger, \tag{2.34}$$

because then we have

$$O_q \begin{pmatrix} \psi_q \\ \psi^\dagger_{-q} \end{pmatrix} = \begin{pmatrix} \chi_q \\ -\chi^\dagger_{-q} \end{pmatrix}. \tag{2.35}$$

However, special care is needed for $k = 0, \pi$ momenta. Since the trigonometric coefficients (2.29) are not well defined, the operators aren't either. Using some rearranged trigonometric expressions of (2.29) (see Appendix (A.3)), we simply define operators χ_q so (A.3b) is fulfilled and take any $\cos\theta_q$ and $\sin\theta_q$ that are consistent with that. The simplest definition of χ_q for $q = 0, N/2$ then is

$$\chi_{q=0} = \psi_{q=0} \tag{2.36a}$$

$$\chi_{q=N/2} = \psi_{q=N/2} \tag{2.36b}$$

It can be shown that operators χ_q are also fermionic and periodic with period N

$$\{\chi_q, \chi_{q'}\} = 0 \tag{2.37a}$$

$$\{\chi_q, \chi^\dagger_{q'}\} = \delta_{qq'}. \tag{2.37b}$$

By reformulating the Hamiltonian (2.21) using operators (2.34) we finally get a diagonal free fermion Hamiltonian

$$H^\pm = \sum_q \Lambda_q \left(\chi^\dagger_q \chi_q - \frac{1}{2} \right). \tag{2.38}$$

2.2 Ground state

Continuing with the solution of the XY model by discussing the ground state, it is important to remind ourselves that the Hamiltonian from 2.1.3 is actually two Hamiltonians, H^+ and H^- and the Hamiltonian that describes our system is actually (2.13). To solve the full Hamiltonian, we need to solve both H^+ and H^-. Each of them have 2^N eigenstates, but as they go into the full Hamiltonian only if they satisfy the parity condition, and that happens half the time for the respective $H^{+,-}$, in the end we will have $2^{N-1} + 2^{N-1} = 2^N$ eigenstates for the full Hamiltonian, exactly as we should.

We will split our solution into two categories multiple times. First, we will look

at the ferromagnetic case for completeness. Then, we will focus on the more interesting case of an antiferromagnetic alignment where we will look separately at the unfrustrated (N is even) and the frustrated (N is odd) case.

The analysis will be made simpler by looking only at the quadrant $(y \geq 0, h \geq 0)$ in the parameter space. It is easy to see that by a $\pi/2$ rotation along the z-axis, a $\gamma \to -\gamma$ equivalent transformation is achieved, whereas a spin reflection across the x-y plane corresponds to $h \to -h$.

2.2.1 Ferromagnetic case

Ferromagnetic order corresponds to a negative coupling constant $J < 0$. For simplicity, we will use $J = -1$. As mentioned, we will look separately at the even and odd sector.

Even sector The ground state of the H^+ Hamiltonian is its vacuum state, which we'll label by $|GS^+\rangle$

$$\chi_q \, |GS^+\rangle = 0 \quad \text{for any } q \in \left\{ \frac{1}{2}, \frac{1}{2}+1, ..., \frac{1}{2}+N-1 \right\}. \tag{2.39}$$

As we can see from (2.38), the ground state energy is given by

$$E_0^+ = -\frac{1}{2} \sum_{q=0}^{N-1} \Lambda_{q+1/2}. \tag{2.40}$$

Wanting to find the explicit expression for the ground state, we start by using operators (2.20) and their property

$$\psi_q \, |0\rangle = 0 \quad \text{for any } q. \tag{2.41}$$

By expanding this equation using (2.37), and using properties of $\sin\theta_q$ and $\cos\theta_q$, we get (see Appendix B)

$$\chi_q(\cos\theta_q + \sin\theta_q \, \psi_q^\dagger \psi_{-q}^\dagger) \, |0\rangle = 0. \tag{2.42}$$

Given equation (2.42), one can check that the ground state of the even sector Hamil-

tonian H^+, normalized, is

$$|GS^+\rangle = \prod_{q=0}^{\left\lfloor \frac{N}{2} \right\rfloor - 1} \left(\cos\theta_{q+1/2} + \sin\theta_{q+1/2}\, \psi^\dagger_{q+1/2} \psi^\dagger_{-(q+1/2)} \right) |0\rangle \,. \tag{2.43}$$

The product goes only up to the $\left\lfloor \frac{N}{2} \right\rfloor - 1$ as the other half of indices would just produce the same state, just with a minus sign in front, resulting in zero.
Moreover, as we can see, the operators ψ_q occur in pairs. By the definition (2.20), that means that ψ_j also occur in pairs, which leads to the $|GS^+\rangle$ (2.43) having even parity. An even parity ground state in the even sector means (2.43) is also an eigenstate of the Hamiltonian (2.13).

Odd sector We proceed analogous to the even sector, but we will label the vacuum state as $|GS^*\rangle$ for reasons that will become clear later

$$\chi_q |GS^*\rangle = 0 \quad \text{for any } q \in \Big\{0, 1, ..., N-1\Big\}. \tag{2.44}$$

We have an analogous situation to the even sector with (2.42), and the ground state for the Hamiltonian H^- is

$$|GS^*\rangle = \prod_{q=0}^{\left\lfloor \frac{N-1}{2} \right\rfloor} \left(\cos\theta_q + \sin\theta_q \psi^\dagger_q \psi^\dagger_{-q} \right) |0\rangle \,. \tag{2.45}$$

As this is essentially the same expression as the ground state of the even sector (2.43), it also has even parity, which means that it gets canceled by the operator $1-P$. Therefore, to find the eigenstate of the full Hamiltonian, we need to add an excitation. If we minimize the expression (2.31) we get that the lowest energy excitation is for $q = 0$, so the common eigenstate of the odd sector and full Hamiltonian with the lowest energy is gained by adding an excitation at $q = 0$ to (2.45)

$$|GS^-\rangle = \chi^\dagger_{q=0} |GS^*\rangle = \psi^\dagger_{q=0} \prod_{q=0}^{\left\lfloor \frac{N-1}{2} \right\rfloor} \left(\cos\theta_q + \sin\theta_q \psi^\dagger_q \psi^\dagger_{-q} \right) |0\rangle \,. \tag{2.46}$$

Let us find the corresponding energies. Here, we will need to differ between $h > 1$ and $h < 1$ (usually it would be $h >$ or $h <$ than J, this is purely because of our choice

$J = -1$). In both scenarios we're starting with the energy of the vacuum, which is equal to the energy of the vacuum (and even sector) E_0^+ (2.40) to which we're adding the contribution of the added Bogoliubov particle with $q = 0$. Remember that, with $J = -1$, that contribution can be positive or negative (see (2.25)).

h > 1.

The contribution is positive, but it is still the minimal possible addition which is necessary to keep parity odd, and the energy is simply

$$E_0^- = -\frac{1}{2}\sum_{q=1}^{N-1}\Lambda_q + \frac{1}{2}(h-1). \tag{2.47}$$

h < 1.

This time the contribution is negative. However, it is possible to neatly incorporate it into the vacuum sum.

$$E_0^- = -\frac{1}{2}\sum_{q=1}^{N-1}\Lambda_q + \frac{1}{2}(h-1), \quad h-1 = -\Lambda_0,$$
$$E_0^- = -\frac{1}{2}\sum_{q=0}^{N-1}\Lambda_q.$$

The corresponding energies are

$$E_0^- = \begin{cases} -\frac{1}{2}\sum_{q=0}^{N-1}\Lambda_q & \text{for } h \leq 1, \\ \\ -\frac{1}{2}\sum_{q=0}^{N-1}\Lambda_q + (h-1) & \text{for } h \geq 1. \end{cases} \tag{2.48}$$

The rest of the eigenstates can be reached by applying the creation operators χ_q in pairs, on states (2.43) and (2.46). This concludes the discussion of the ferromagnetic XY chain.

2.2.2 Antiferromagnetic case

Moving onto antiferromagnetic order and setting $J = 1$, we will first need to construct the parameter space of the system (h, γ). As we will see, for a certain combina-

tion of parameters there will appear new local minima or maxima, which are directly related to frustration and will lead to a difference in ground state in regards to the unfrustrated (and ferromagnetic) case. Moreover, the special momenta $k = 0, \pi$ will switch places, further complicating things and allowing for frustration to occur. Table 2.1 classifies the placement of the modes across sectors and for different N.

N	sector	0	π
even	even	$\times$	$\times$
	odd	✓	✓
odd	even	$\times$	✓
	odd	✓	$\times$

Table 2.1: The distribution of $k = 0, \pi$ modes over sectors for different N in the antiferromagnetic ordering.

Considering J is now positive, we have a slightly altered energy function Λ_k, so we need to check the stationary points of this new function in order to be able to construct the ground state of the system across sectors. The function Λ_k is now

$$\Lambda_k = \sqrt{(h + \cos k)^2 + \gamma^2 \sin^2 k}. \tag{2.49}$$

Along with two familiar points analogous to the ferromagnetic case, $k = 0, \pi$, another one emerges. Or, to be precise, since it's no longer a limiting point which has no opposite value like the first two, two new extremes emerge.

$$k_1 = 0, \tag{2.50a}$$

$$k_2 = \pi, \tag{2.50b}$$

$$\pm k^* = \pm \arccos \frac{h}{\gamma^2 - 1}. \tag{2.50c}$$

Because k^* is defined over a $\arccos$, it exists only for

$$|h| \leq |\gamma^2 - 1|. \tag{2.51}$$

The equality in this inequality defines a parabola which will prove to be crucial in the analysis of this model.

Even N For even N, the antiferromagnetic case barely differs from the ferromagnetic case (2.2.1). The only difference is that the energies of $k = 0$ and $k = \pi$ modes switch places, so $k = \pi$ is now the minimum instead of $k = 0$. However, that is not a problem since, again, both momenta are in the odd sector (2.1). Therefore, in the odd sector the excitation we add is for $k = \pi$ instead of 0, but the energy remains the same. The ground states and energy spectra are given here

$$|GS^+\rangle = \prod_{q=0}^{\left\lfloor \frac{N}{2} \right\rfloor - 1} \left(\cos\theta_{q+1/2} + \sin\theta_{q+1/2}\, \psi^\dagger_{q+1/2} \psi^\dagger_{-(q+1/2)} \right) |0\rangle \,, \tag{2.52}$$

$$|GS^-\rangle = \chi^\dagger_{q=\pi} \prod_{q=0}^{\left\lfloor \frac{N-1}{2} \right\rfloor} \left(\cos\theta_q + \sin\theta_q \psi^\dagger_q \psi^\dagger_{-q} \right) |0\rangle \,. \tag{2.53}$$

and the energies are, in the end, completely the same

$$E_0^+ = -\frac{1}{2} \sum_{q=0}^{N-1} \Lambda_{q+1/2}, \tag{2.54}$$

$$E_0^- = \begin{cases} -\frac{1}{2} \sum_{q=0}^{N-1} \Lambda_q & \text{for } h \leq 1, \\ -\frac{1}{2} \sum_{q=0}^{N-1} \Lambda_q + (h-1) & \text{for } h \geq 1. \end{cases} \tag{2.55}$$

Odd N We have reached the final scenario. Since we have periodic boundary conditions, antiferromangetic coupling and now also an odd number of spins in a chain, we have all the conditions necessary for frustration to arise. As we will see, the presence of frustration will depend on the combination of parameters h and γ.

On account of that fact, we will approach the search for the ground state by dividing the parameter space into four regions. See Figure 2.1 for illustration of the parameter space with all the main parameter configurations.

Even sector The Hamiltonian of the even sector in this case is the following

$$H^+ = \sum_{x \in X_+ \setminus N/2} \Lambda_q \left(\chi^\dagger_q \chi_q - \frac{1}{2} \right) + (h-1) \left(\chi^\dagger_{N/2} \chi_{N/2} - \frac{1}{2} \right), \tag{2.56}$$

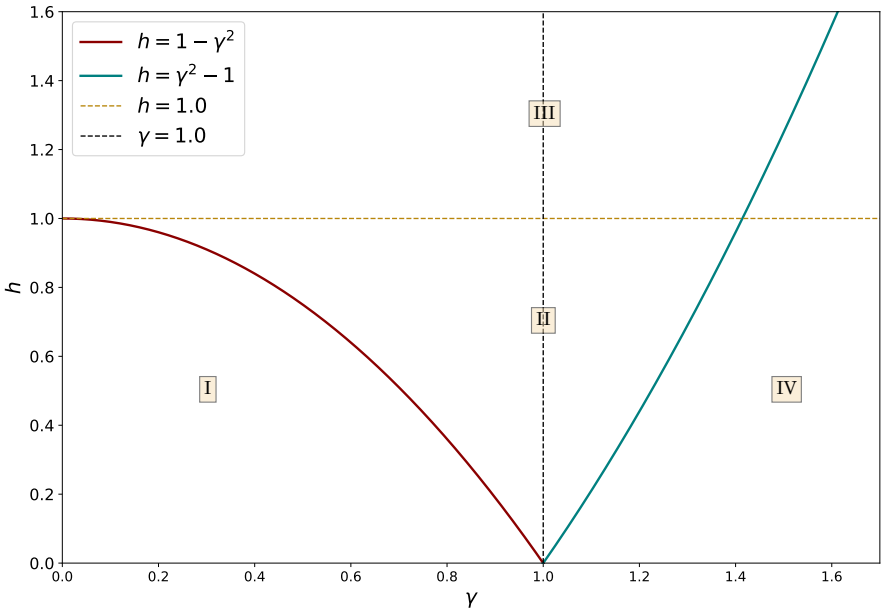

Figure 2.1: An illustration of the parameter space. Red and blue lines depict the parabola under which the special momenta $\pm k^*$ exists. $h = 1.0$ is also an important line as it affects the sign of the $k = 0.\pi$ energies whereas $\gamma = 1.0$ was added for completeness. The regions noted $I - IV$ will be used in the analysis of the ground state.

with:

$$X_+ = \left\{ \frac{1}{2}, \frac{1}{2} + 1, ..., \frac{1}{2} + N - 1 \right\}.$$

We have extracted the π mode to further emphasize its specific energy.

So far, in the even sector we were content with the vacuum as the ground state. It had correct parity and by no excitations, the lowest energy. This is no longer the only option.

Let us look at the graph of the function of energy Λ_k. We will look at the absolute value of the function, and in that way we will also include the values of the energy for $k = \pi$ ($k = 0$ is no longer in this sector).

As we can see from the Figure 2.2, for a certain combination (h, γ), two local extremes appear with momenta $k = \pm k^*$. The interesting situation is when those extremes are minima, corresponding to region I from 2.1, whereas the maxima version corresponds to region IV. In regions II and III the Λ_k function will take shape of the top graph.

Before dwelling into that scenario, we will look at the other regions, as they still

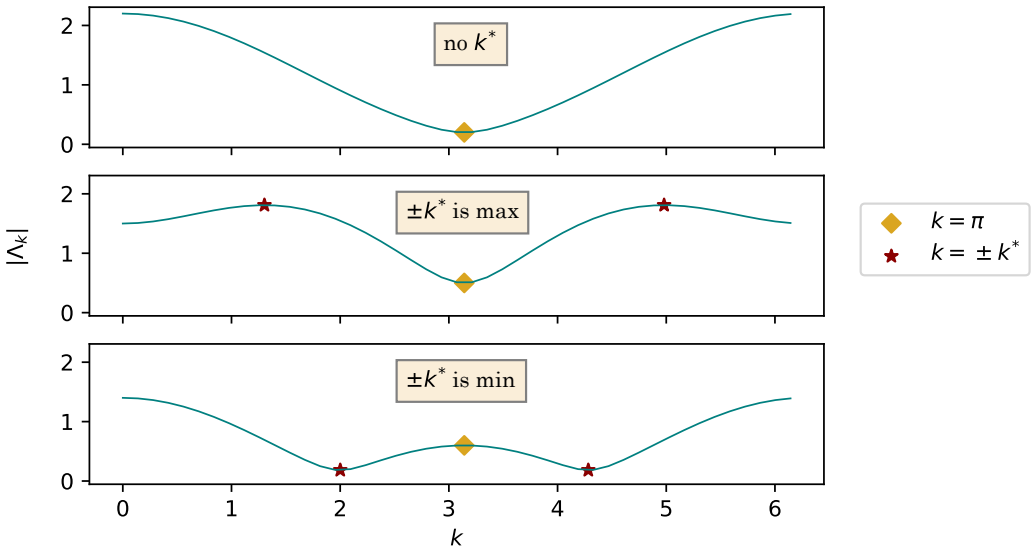

Figure 2.2: These graphs demonstrate how the λ_k function behaves for different configuration of parameters h and γ. The absolute value is put over Λ to emphasize we're comparing absolute values of energies, which is important because of the π mode. The top graph displays the Λ_k function in regions II and III, whereas the middle graph corresponds to region IV. The bottom graph showcases the behaviour which is behind the peculiar nature of region I.

mostly similar to the even N chain 2.2.2. For regions $II - IV$ we can "copy" what we did so far and recognize the vacuum as the ground state.

$$|GS^{+}_{II,III}\rangle = \prod_{q=0}^{\left\lfloor \frac{N}{2} \right\rfloor - 1} \left(\cos\theta_{q+1/2} + \sin\theta_{q+1/2}\, \psi^{\dagger}_{-(q+1/2)} \psi^{\dagger}_{q+1/2} \right) |0\rangle \,. \tag{2.57}$$

The reason why the area is split into different regions will become clear as we look at the energy of the vacuum. If we recall (2.66), we can see that the energy (vacuum energy, regardless of there being an excitation or not)of the π mode ($q = \frac{N}{2}$) can be negative for $h \leq 1$. That is why we divide into regions although the ground state is the same. Furthermore, since both regions II and IV are located under the $h = 1$ line, we can merge the two regions into region II' and conclude that the parabola $h = \gamma^2 - 1$ does not represent any relevant curve, at least for the ground state analysis.

Again starting with the simpler area, for $h \geq 1$ we have region III, where the energy of the π mode is positive. It is actually equal to the value of the Λ_k function for $k = \pi$ and as such can be naturally incorporated into the sum, thereby achieving

a "normal" vacuum energy

$$E_{III} = -\frac{1}{2}\sum_{q=0,q\neq N/2}^{N-1}\Lambda_{q+\frac{1}{2}} - \frac{1}{2}(h-1), \tag{2.58}$$

$$E_{III} = -\frac{1}{2}\sum_{q=0}^{N-1}\Lambda_{q+\frac{1}{2}}, \tag{2.59}$$

where in the last line we used

$$(h-1) = |h-1| = \Lambda_\pi.$$

The reason we say this is "normal" vacuum energy is because in the newly-merged region II' the ground state is the vacuum but the energy exhibits different behaviour which is the following

$$E_{II'} = -\frac{1}{2}\sum_{q=0,q\neq N/2}^{N-1}\Lambda_{q+\frac{1}{2}} - \frac{1}{2}(h-1), \tag{2.60}$$

$$E_{II'} = -\frac{1}{2}\sum_{q=0}^{N-1}\Lambda_{q+\frac{1}{2}} + |h-1|, \tag{2.61}$$

$$E_{II'} = -\frac{1}{2}\sum_{q=0}^{N-1}\Lambda_{q+\frac{1}{2}} + \Lambda_\pi, \tag{2.62}$$

since now

$$(h-1) = -|h-1| = -\Lambda_\pi.$$

This is a significant result since it shows that although the ground state is the vacuum and there is no excitation, the system behaves as if there is an excitation of a Bogoliubov particle with momentum $k = \pi$. This is frustration in effect.

Now is the time for the most special region, the region I under the parabola $h = 1 - \gamma^2$. In this region the condition for $\pm k^*$ is fulfilled. Even further, the $\pm k^*$ are minima, corresponding to the third plot in Figure 2.2.
Turns out, it is possible to create a combination of excitations (a pair) which will simultaneously preserve parity and achieve energy lower than having no excitations at all. How is that possible?

The answer lies in the π mode energy. If you carefully look at the third plot of Figure 2.2, you can see the absolute value of π mode energy, or the Λ_π is greater

than the (degenerate) energies of $\pm k^*$. Because region I is below the $h = 1$ line, this energy is in reality negative. If we add a k^* excitation along with a π excitation we have successfully obtained a lower energy than a simple vacuum state would have. One could argue that it is not a given that the k^* mode is necessary in the even sector. However, that is not an issue, since in that case we would just add the closest momenta to k^* which is the minimum in that sector. Furthermore, since k^* and $-k^*$ modes are degenerate, we actually have a linear combination for a ground state. Considering they are perfectly symmetric, is is enough to simply give them the same weight which also normalizes the state. The ground state in region I is then

$$|GS^+, I\rangle = \frac{1}{\sqrt{2}}\left(\chi_\pi^\dagger \chi_{k^*}^\dagger + \chi_\pi^\dagger \chi_{-k^*}^\dagger\right) \prod_{q=0}^{\left\lfloor \frac{N}{2} \right\rfloor - 1} \left(\cos\theta_{q+1/2} + \sin\theta_{q+1/2}\, \psi_{q+1/2}^\dagger \psi_{-(q+1/2)}^\dagger\right) |0\rangle \,. \tag{2.63}$$

The energy of this state again behaves a bit differently than the actual situation. The π excitation is absorbed into the sum, and the energy seems to show only the $\pm k^*$ excitation

$$E_I = -\frac{1}{2} \sum_{q=0, q\neq N/2}^{N-1} \Lambda_{q+\frac{1}{2}} - \frac{1}{2}(h-1) + (h-1) + \Lambda_*, \tag{2.64}$$

$$E_I = -\frac{1}{2} \sum_{q=0}^{N-1} \Lambda_{q+\frac{1}{2}} + \Lambda_*. \tag{2.65}$$

The system would rather have an excitation (or two to be precise), than be in a vacuum state - this is the consequence of frustration.

However, it is not this simple. It must not be overlooked that k^* directly depends on h and γ (2.50c). Any change in the parameters that does not preserve the relation $\cos k^* = \frac{h}{\gamma^2 - 1}$ implies a different k^*, signifying sort of a continuous series of level-crossings signifying each change. More on that later.

Odd sector The Hamiltonian of the odd sector is

$$H^+ = \sum_{x \in X_- \setminus 0} \Lambda_q \left(\chi_q^\dagger \chi_q - \frac{1}{2}\right) + (h-1)\left(\chi_0^\dagger \chi_0 - \frac{1}{2}\right), \tag{2.66}$$

with

$$X_+ = \{0, 1, ..., N-1\}\,.$$

To find the ground state in the odd sector, we need to know which momentum excitation will lead to the lowest energy increase. It is impossible to achieve a lower energy, as the only negative contribution would come from the π mode, which is not in this sector. Considering the energy function Λ_q shown in 2.2 is valid for the whole antiferromagnetic case, it is easy to recognize the minima, or to be more precise, the minimal values of Λ in different areas of the parameter space. The problem is that the π momentum has the lowest energy everywhere for $h > 1-\gamma^2$. Since we cannot take that momentum, we will take second best. Turns out the Λ_k function is symmetric based on $k = \pi \rightarrow q = \frac{N}{2}$, so these "second-best" will be doubly-degenerate (see Figure 2.3).

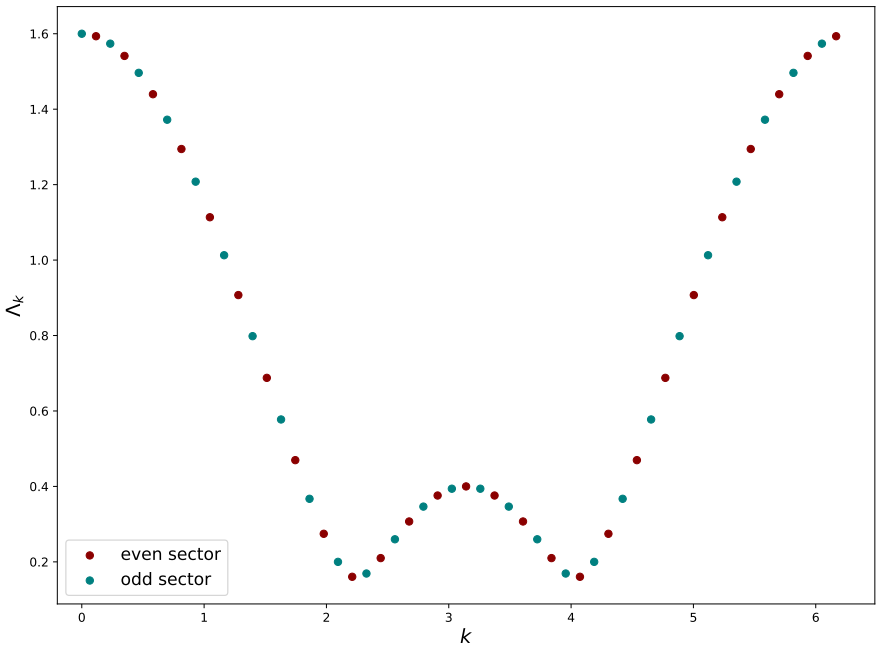

Figure 2.3: The available momenta in the even and odd sector respectively for $N = 27$. It is easy to see the peak centered on $k = \pi$ has symmetric points in both sectors, leading to a double-degeneracy when the π mode is not in the needed sector. Also, it can be seen that around the peaks of $\pm k^*$ the distribution of points is asymmetrical which confirms that there is no degeneracy when adding the closest momenta to k^* as in the even sector.

We will split the parameter space in only two regions, as we're only interested in

the minima and for that we have two options.

Under the parabola $h < 1-\gamma^2$ will be area A (using A and B will help differentiate from the even sector solutions) and there the minima are $\pm k^*$ respectively. In the case $\pm k^*$ are not in the odd sector, the reasoning is the same as in the even sector: for sure there is a unique (for each well) minimum so we will just take those points (see Figure 2.3 for proof), but for simplicity we will stick with the notation of k^*. The ground state is then

$$|GS_A^-\rangle = \frac{1}{\sqrt{2}}\left(\chi_{k^*}^\dagger + \chi_{-k^*}^\dagger\right)\prod_{q=0}^{\left\lfloor\frac{N}{2}\right\rfloor-1}\left(\cos\theta_{q+1/2} + \sin\theta_{q+1/2}\,\psi_{q+1/2}^\dagger\psi_{-(q+1/2)}^\dagger\right)|0\rangle \quad (2.67)$$

Region B comprises of the are above the parabola $h > 1-\gamma^2$ where π is the minimum. As mentioned, here we are unable to excite the π mode so we need to take the next in line, which introduces degeneracy

$$|GS_B^-\rangle = \frac{1}{\sqrt{2}}\left(\chi_{\frac{N-1}{2}}^\dagger + \chi_{\frac{N+1}{2}}^\dagger\right)\prod_{q=0}^{\left\lfloor\frac{N}{2}\right\rfloor-1}\left(\cos\theta_{q+1/2} + \sin\theta_{q+1/2}\,\psi_{q+1/2}^\dagger\psi_{-(q+1/2)}^\dagger\right)|0\rangle \quad (2.68)$$

The energy is then simply given by the vacuum energy plus the excitations we have added

$$E_0^- = \begin{cases} -\frac{1}{2}\sum_{q=0}^{N-1}\Lambda_q + \Lambda_*, & A : h \le 1-\gamma^2 \\ -\frac{1}{2}\sum_{q=0}^{N-1}\Lambda_q + \Lambda_{\frac{N-1}{2}}, & B : h > 1-\gamma^2 \end{cases} \quad (2.69)$$

The true ground state of the system switches between odd and even sectors moving through the parameters. However, very quickly with increasing N the energies of the sectors entwine closer and closer together, especially rapidly for the frustrated region (see Figure 2.4). Already for $N > 10$ they are very similar (depending on the fixed parameter of course) and since we're interested essentially in the thermodynamic limit, we will assume degeneracy and only look at the even sector most of the time.

This concludes the solution of the one-dimensional quantum XY model.

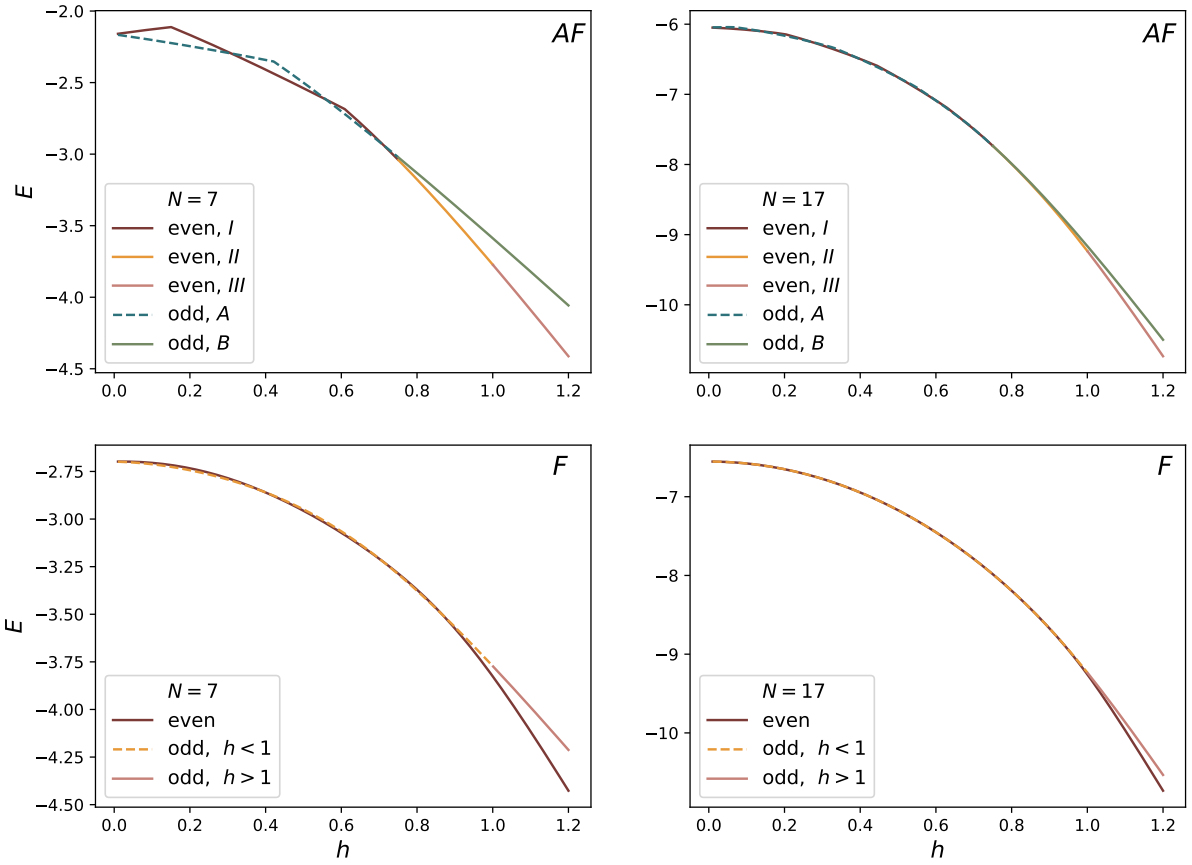

Figure 2.4: The energies of different sectors for the ferromagnetic (F) and antiferromagnetic (AF) coupling with different chain lengths. We see even for still quite short chains, the energies are very similar, especially in the region of interest $h < 1$. All four graphs energies have been calculated for $\gamma = 0.5$.

3 Fidelity

Fidelity is a function of overlap between two quantum states. By measuring the similarity between two states corresponding to systems with slightly different parameters, fidelity can be used to effectively identify critical points by recognizing the orthogonality emerging at those points, which is (often) a signature of QPTs. Given two quantum states described by density operators ρ and σ, fidelity is defined as [22]

$$\mathcal{F}(\rho, \sigma) \coloneqq \mathrm{tr}\left(\sqrt{\rho^{1/2}\sigma\rho^{1/2}}\right). \tag{3.1}$$

In the case of pure states, (3.1) reduces to the overlap between two states. Given

$\rho = |\psi_Z\rangle \langle\psi_Z|$ and $\sigma = |\psi_{\tilde{Z}}\rangle \langle\psi_{\tilde{Z}}|$, the fidelity of pure states is then

$$\mathcal{F}(Z, \tilde{Z}) = |\langle\psi_Z|\psi_{\tilde{Z}}\rangle|. \tag{3.2}$$

By this notation, we presume Z and $\tilde{Z}$ are two states with parameters differing by a (not necessarily infinitesimal) small step $(h, \gamma) \to (h + dh, \gamma + d\gamma)$.

As was mentioned in Section 1, it will be necessary to slightly alter our approach by introducing a partial measurement called reduced fidelity to fully characterize our system due to the specific geometry in the frustrated region causing exact orthogonality. This implies using reduced density matrices in place of "regular" full-system density matrices which will entail calculating the necessary, in this case, two-point correlation functions. Since we will be calculating also reduced fidelity, we will refer to the "regular" fidelity as global fidelity.

3.1 Global fidelity

The global fidelity will be evaluated for the vacuum states (F_0), states with one excitation (F_1) and for the doubly excited, doubly degenerated states (F_2). The former will cover the fidelity for the ferromagnetic chain for $h > 1$, and the fidelity in the antiferromagnetic regions II' and III. The state with one excitation is the ground state of the ferromagnetic $h < 1$ region and the former is important for the frustrated region I of the antiferromagnetic chain. The reason why we only look at the fidelity between states with an equal number of excitations is that we are interested only in parameter-induced differences in ground states, since they are the ones who are supposed to signal the presence of a phase transition. "Regular" orthogonalities between fundamentally distinct states such as states with a different number of excitations are of no interest to us; their overlaps vanish even for identical parameters.

3.1.1 Analytical expression

Vacuum To help obtain the fidelity, we will use an equivalent but slightly different way of expressing the vacuum state

$$|vac\rangle = \bigotimes_{q=0}^{\left\lfloor \frac{N}{2} \right\rfloor - 1} \cos\theta_{q+\frac{1}{2}} |0\rangle_{q+\frac{1}{2}} |0\rangle_{-\left(q+\frac{1}{2}\right)} + \sin\theta_{q+\frac{1}{2}} |1\rangle_{q+\frac{1}{2}} |1\rangle_{-\left(q+\frac{1}{2}\right)}. \tag{3.3}$$

Using this notation, it is pretty straightforward to obtain the overlap

$$\mathcal{F}_0 = |\langle vac|\, \widetilde{vac}\rangle| \tag{3.4}$$

$$= \prod_{q=0}^{\left\lfloor \frac{N}{2} \right\rfloor - 1} \left(\cos\theta_{q+\frac{1}{2}} \cos\tilde{\theta}_{q+\frac{1}{2}} + \sin\theta_{q+\frac{1}{2}} \sin\tilde{\theta}_{q+\frac{1}{2}} \right). \tag{3.5}$$

The vacuum fidelity is then

$$\mathcal{F}_0 = \prod_{q=0}^{\left\lfloor \frac{N}{2} \right\rfloor - 1} \cos\left(\theta_{q+\frac{1}{2}} - \tilde{\theta}_{q+\frac{1}{2}} \right). \tag{3.6}$$

One excitation Moving on to states with one excitation, we will look first at a general excitation Q. The fidelity we want to calculate is then

$$\mathcal{F}_1 = |\, \langle vac|\, \chi_Q\, \tilde{\chi}_Q\, |\widetilde{vac}\rangle\, |. \tag{3.7}$$

The idea is to use the definition of the χ_q operators (2.34), as well as the recently introduced notation for the vacuum state (3.3) to expand the expression and (2.9) to simplify and obtain the end result (see Appendix C.1 for details)

$$\mathcal{F}_1 = \prod_{q=0, q\neq Q}^{\left\lfloor \frac{N-1}{2} \right\rfloor} \cos\left(\theta_q - \tilde{\theta}_q \right). \tag{3.8}$$

Of course, if we're only interested in true ground state fidelity, the momentum $Q = 0$ as it corresponds to the ground state of the ferromagnetic chain for $h < 1$. However, we will see it will prove to be useful to have done this calculation for the general momentum Q.

Two excitations Before calculating the fidelity of the ground state (2.63), it is crucial to take into account that the $\pm k^*$ momenta depends on parameters h and γ, thereby greatly affecting the overlap of the two states.
The following expression clearly states the issue

$$\cos k^* = \frac{h}{\gamma^2 - 1}. \tag{3.9}$$

As soon we change h or γ, no matter by how little, we obtain a different momentum and therefore excite a different Bogoliubion particle, effectively rendering the fidelity exact zero

$$\mathcal{F}_2^a = \langle GS_2 | \widetilde{GS}_2 \rangle = 0, \quad k^* \neq, \tilde{k^*} \tag{3.10}$$

where we use $|GS_2\rangle$ as a shorter notation for the ground state (2.63).
The only way to avoid this is to keep the ratio in (3.9) constant, which entails moving along a family of parabolas

$$h = c(1 - \gamma^2), \tag{3.11}$$

keeping $c \in [-1, 1]$ constant for a specific k^*.

Because of this peculiar geometry, it is reasonable to introduce different variables, i.e. natural variables. Parameter c already imposed itself as one. It will define the direction tangent to the parabola, i.e. varying c moves along a parabola. By some manipulation it is possible to obtain also the normal direction, let's denote it by δ (see Appendix C.2).

$$\begin{cases} c = \frac{h}{1-\gamma^2}, & -1 \leq c \leq 1 \\ \delta = -\frac{\gamma^2}{2} - h^2 + \ln \gamma, & \delta \geq -\ln \gamma + \frac{\gamma^2}{2}. \end{cases} \tag{3.12}$$

However, to obtain the formula itself we don't need to specify which parameters we are using just yet. We're looking at the expression

$$\mathcal{F}_2 = \frac{1}{2} \Big| \langle vac | \chi_\pi \Big(\chi_{k^*} + \chi_{-k^*} \Big) \Big(\tilde{\chi}^\dagger_{k^*} + \tilde{\chi}^\dagger_{-k^*} \Big) \tilde{\chi}_\pi \, | \widetilde{vac} \rangle \Big| \tag{3.13}$$

$$= \frac{1}{2} \Big| \langle vac | \Big(\chi_{k^*} \tilde{\chi}^\dagger_{k^*} + \chi_{k^*} \tilde{\chi}^\dagger_{k^*} \Big) | \widetilde{vac} \rangle \Big|. \tag{3.14}$$

Looking at the first line, we can start by eliminating the cross products containing both k^* and $-k^*$ as those states will definitely differ and be orthogonal regardless of the change in parameters since they will simply have different excitations.
Another piece brings us to the next line, and that is the fact that the π excitation proves to be irrelevant overlap-wise. Since for $k = \pi$ there is no rotation, there is no dependence on parameters

$$\tilde{\chi}_\pi = \chi_\pi = \psi_\pi. \tag{3.15}$$

There is no acquired phase (it is $+1$) from (2.9) so what is left in (3.14) is basically

a one excitation fidelity which we have already calculated in (3.8) so the result is

$$\mathcal{F}_2 = \prod_{q=0,\, \frac{2\pi q}{N} \neq k^*}^{\left\lfloor \frac{N}{2} \right\rfloor - 1} \cos\left(\theta_{q+\frac{1}{2}} - \tilde{\theta}_{q+\frac{1}{2}}\right) \delta_{k^* \tilde{k}^*}. \tag{3.16}$$

The $\delta_{k^*\tilde{k^*}}$ function is there to remind us that this expression is only valid if we keep k^* constant while varying h and γ.

3.1.2 Results

The global fidelity is always given by a product of cosines of the difference of Bogoliubov angles. The only thing that differs in non-vacuum states is that the momenta which are excited are omitted from the product. However, while the overlap of vacuum states exhibits fairly smooth behaviour, the two excitation overlap abruptly drops to zero every time k^* changes, displaying a highly singular nature.

Based on these expressions, we produced graphs showing the behaviour of global fidelity across the parameter space, with keeping one parameter constant and varying the other. For ferromagnetic order, the fidelity clearly shows the expected peaks at the well known $h = 1$ Ising transition (see Figure 3.1) and $\gamma = 0$ XX transition points (see Figure 3.2). Both graphs display that the peak sharpens and increases with increasing N. This is a signature of the fact that in the thermodynamic limit $N \to \infty$ this dip becomes a real discontinuity. The parity of N plays no role here, as for the ferromagnetic order there can be no frustration. The global fidelity of antiferromagnetic order for even N show the same behaviour. Both of these cases correspond to either vacuum or 0 or π excitations states, depending on parameters, as per 2.2.1 and 2.2.2.

New cases arise when we move into frustrated territory. As we found in 2.2.2 Odd N paragraph, the ground state for $h < 1 - \gamma^2$ is either vacuum excited only by k^* or both k^* and π. Furthermore, in region dubbed II' in the 2.2.2 paragraph we have frustrated vacuum (vacuum that acts as if there is a π excitation in its energy). Concentrating on the first scenario involving a k^* excitation, we encounter the already mentioned issue. As k^* changes going through the parameters h and γ the fidelity drops to zero identically as the two states become orthogonal. Then, moving out of region I/A the fidelity shots back up near the value of 1, dropping again at the Ising

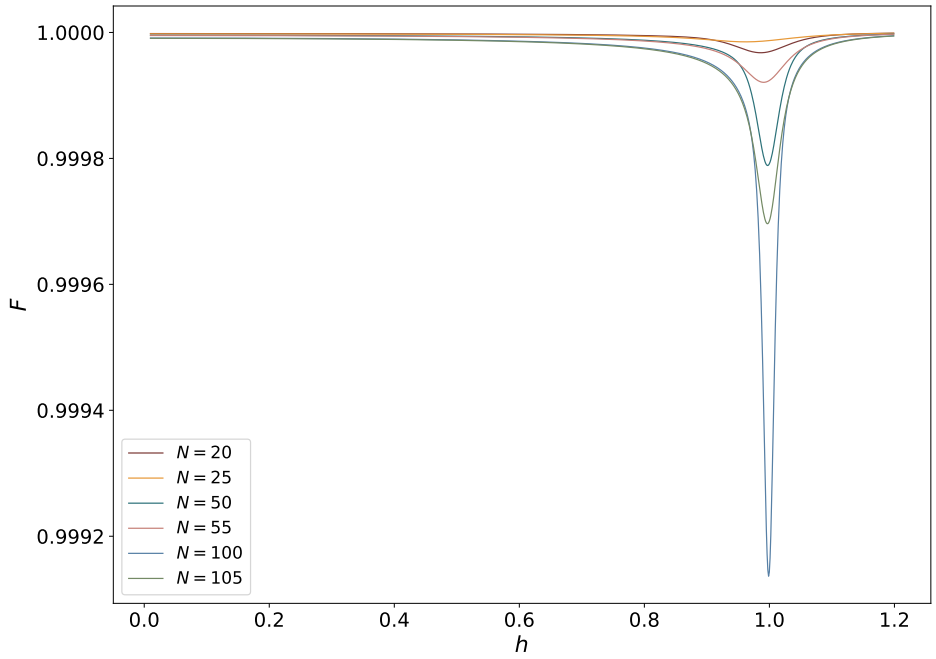

Figure 3.1: Fidelity in the case of ferromagnetic order $J = -1$ with fixed anisotropy $\gamma = 0.5$ in range $h = [0.01, 1.2]$. A clear dip is seen at $h = 1.0$ that increases with increasing N.

transition $h = 1$ (or the $\gamma = 0$ when varying γ). The described situation is displayed in Figure 3.3 for variation of h and in Figure for variation of γ.

This fact is further affirmed in Figure 3.5. When γ is varied not for fixed h, but along a specific parabola (3.11), the discontinuities encountered when moving in other directions are avoided and we're left with a clear drop signalling only the $\gamma = 0$ transition.

The aforementioned drops in the fidelity and shown in 1D variations of h and γ separately are further corroborated in 3.6, which clearly demonstrates that fidelity can be used to (re)-construct a phase diagram of a system.

3.1.3 Fidelity susceptibility

The definition of fidelity given by (3.2) implies a subtle dependence on the size of steps used to move in parameter space dh and $d\gamma$. However, it is possible to avoid that by looking at fidelity susceptibility [9]. If we write more explicitly the aforementioned dependence we can expand the fidelity around the starting parameters

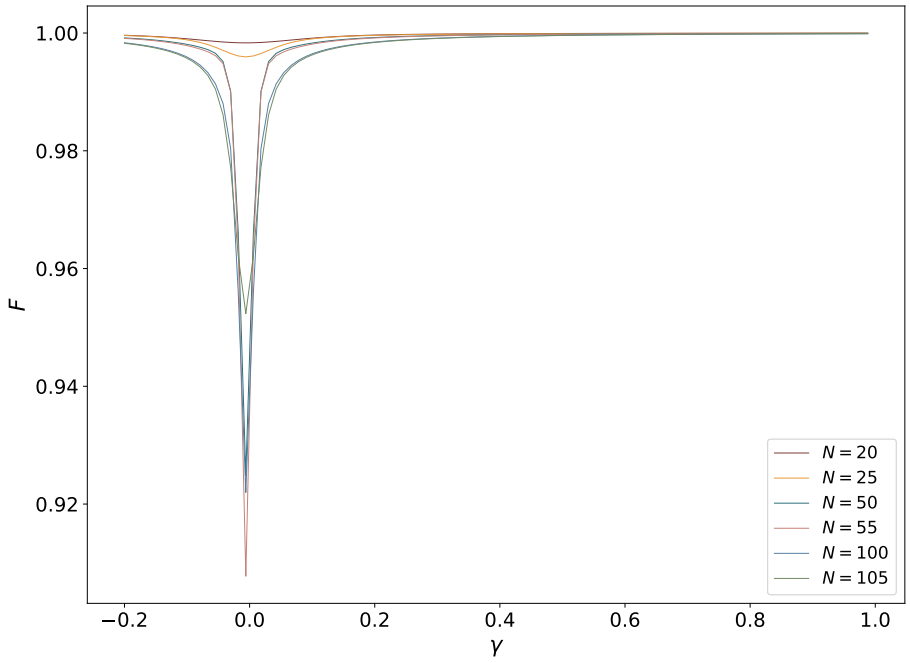

Figure 3.2: Fidelity in the case of ferromagnetic order $J = -1$ with fixed magnetic field $h = 0.6$ in range $\gamma = [-0.2, 1.0]$. A clear dip is seen at $\gamma = 0.0$ that increases with increasing N.

(h, γ).

$$\mathcal{F} = \prod_{q'} \cos\left[\theta_{q'}(h + dh, \gamma + d\gamma) - \theta_{q'}(h, \gamma)\right]. \tag{3.17}$$

We expand first the argument of the cosine up to first order but also the cosine itself, to second order:

$$= \prod_{q'} \cos\left(-\frac{\partial\theta_{q'}}{\partial h}h - \frac{\partial\theta_{q'}}{\partial\gamma}\right), \tag{3.18}$$

$$\approx \prod_{q'} \left[1 - \frac{1}{2}\left(\frac{\partial\theta_{q'}}{\partial h}h + \frac{\partial\theta_{q'}}{\partial\gamma}\gamma\right)^2\right]. \tag{3.19}$$

Now, writing it in in a shorter fashion

$$\mathcal{F} = 1 + \frac{1}{2}\sum_{i,j} g_{ij} d\lambda_i d\lambda_j, \tag{3.20}$$

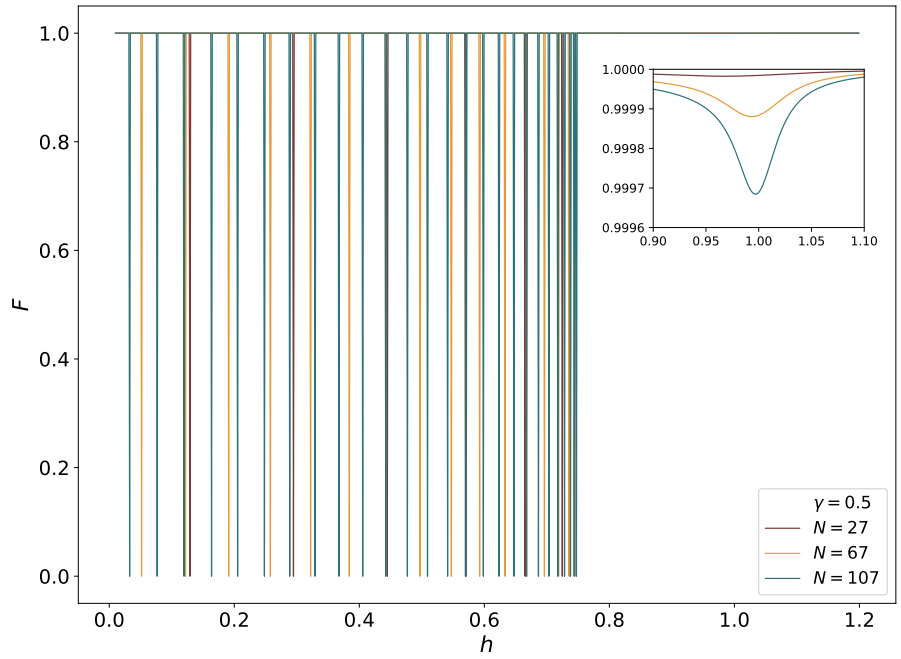

Figure 3.3: Fidelity in the case of antiferromagnetic order $J = +1$ with fixed anisotropy $\gamma = 0.5$ in range $h = [0.1, 1.2]$. We see multiple discontinuities where $F = 0$, whose number is increasing with N. The Ising peak $h = 1.0$ is still there.

where the sum i, j goes over available parameters, in this case h and γ. g_{ij} is the metric tensor and its components are fidelity susceptibilities:

$$g_{i,j} = -\sum_{q'} \partial_i \theta_{q'} \, \partial_j \theta_{q'}. \tag{3.21}$$

q' is used as a wrap notation for all versions of the available momenta.

The quantum metric tensor is symmetric under exchange of the index i and j. It is the real part of a more generalized quantum geometric tensor of the ground state. By taking the thermodynamic limit the sum can be replaced by an integral $\sum_{k'} \to [N/(2\pi)] \int_0^\pi dx$. These integrals are then calculated using complex integration. Then, the components of the metric tensor, with a switch to an intensive quantity

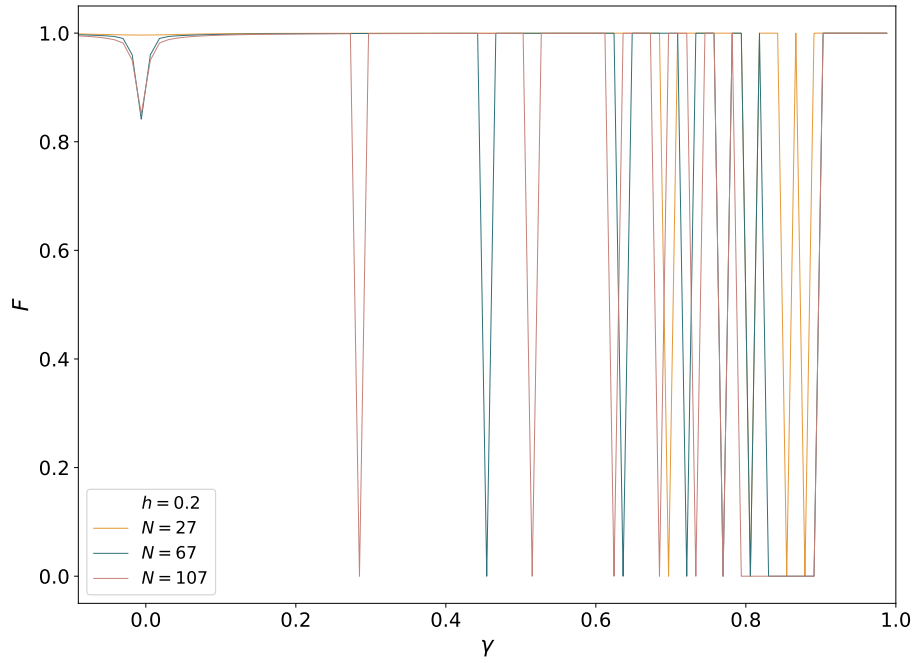

Figure 3.4: Fidelity in the case of antiferromagnetic order $J = +1$ with fixed magnetic field $h = 0.2$ in range $\gamma = [-0.1, 1.0]$. We see multiple discontinuities where $F = 0$, whose number is increasing with N. The $\gamma = 0$ peak is still there.

$g_{ij} \to q_{ij}/N$, are given by

$$g_{hh} = \frac{1}{16}\begin{cases} \frac{1}{|\gamma|(1-h^2)}, & |h| < 1 \\ \frac{|h|\gamma^2}{(h^2-1)(h^2-1+\gamma^2)^{3/2}}, & |h| > 1 \end{cases} \tag{3.22a}$$

$$g_{\gamma\gamma} = \frac{1}{16}\begin{cases} \frac{1}{|\gamma|(1+|\gamma|)^2}, & |h| < 1 \\ \left[\frac{2}{(1-\gamma^2)^2}\left(\frac{|h|}{\sqrt{h^2-1+\gamma^2}} - 1\right) - \frac{|h|\gamma^2}{(1-\gamma^2)(h^2-1+\gamma^2)^{3/2}}\right], & |h| > 1 \end{cases} \tag{3.22b}$$

$$g_{h\gamma} = \frac{1}{16}\begin{cases} 0, & |h| < 1 \\ \frac{-|h|\gamma}{h(h^2-1+\gamma^2)^{3/2}}, & |h| > 1 \end{cases} \tag{3.22c}$$

However, because of continuous divergences in region I of the antiferromagnetic chain $h < 1 - \gamma^2$, it is important to notice that these expressions are not valid in this region; we will need a different approach. Since the fidelity function is not analytical we cannot even define the second derivative in general. Nonetheless, we can define it moving strictly along each parabola given by (3.11). Keeping c a parameter which chooses which parabola we're on, we have a relation how h changes for a given γ.

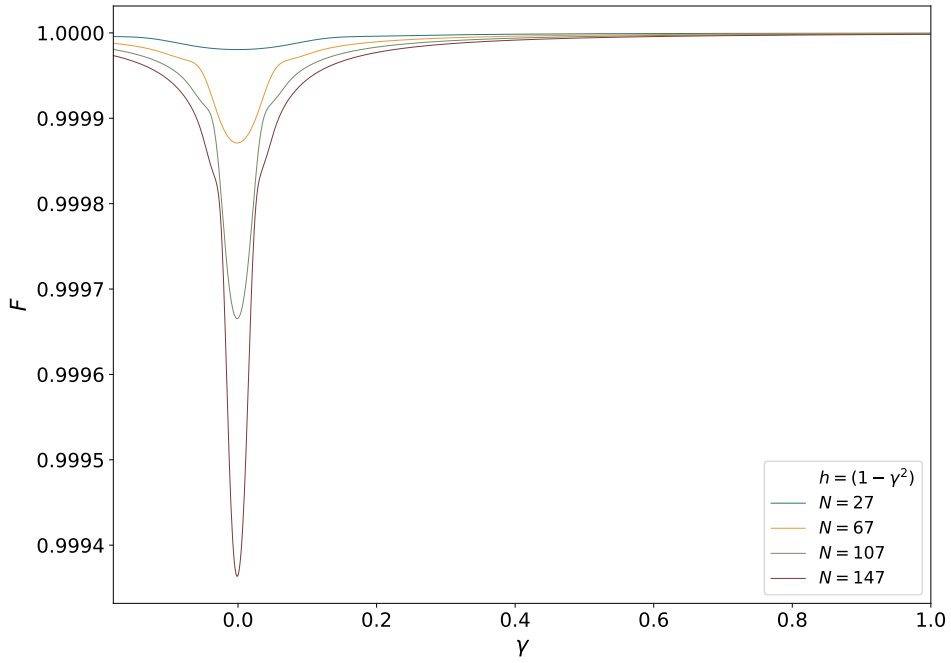

Figure 3.5: Fidelity in the case of antiferromagnetic order $J = +1$ with varying γ in range $[-0.1, 1.0]$. along parabola $h = 1 - \gamma^2$

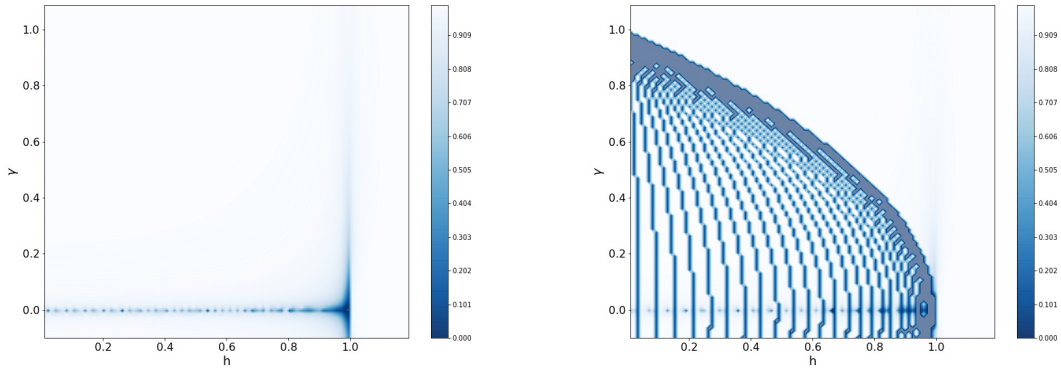

(a) Parameter space vs. fidelity for $J = -1$, $N = 207$.

(b) Parameter space vs. fidelity for $J = 1$, $N = 107$.

Figure 3.6: Simultaneous varying of both h and γ displayed in the contour technique for a) Ferromagnetic b) Antiferromagnetic order. Although $h = 1$ is less strong than the rest, the graphs clearly show the drops in fidelity occurring for all the expected parameters, $h = 1$, $\gamma = 0$ and the k^* level-crossings. In Figure C.1 you can see how the continuous limit takes place, already for $N = 507$.

By using $h = c(1 - \gamma^2)$ in our definition of θ_q (A.3a) we obtain the susceptibility for region I. Let us denote it as $\tilde{g}_{\gamma\gamma}$ to differentiate from the "normal" susceptibility

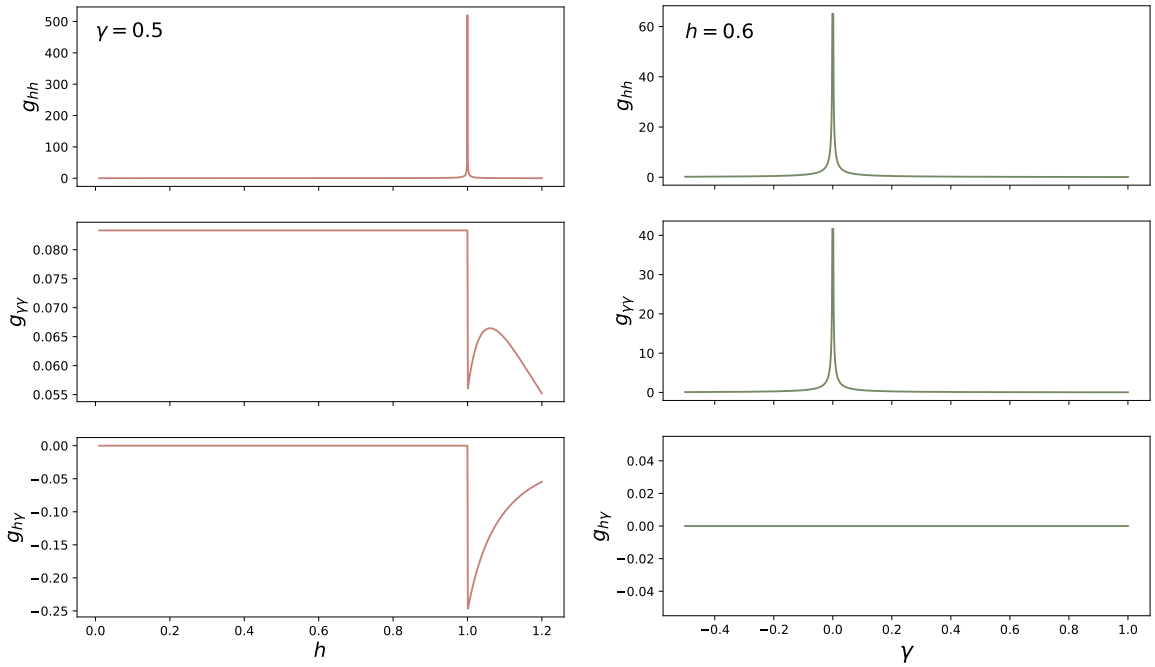

(a) Fidelity susceptibilities $g_{ij}(h)$ for $\gamma = 0.5$. (b) Fidelity susceptibilities $g_{ij}(\gamma)$ for $h = 0.6$.

Figure 3.7: Illustration of each component of the metric tensor by varying h and γ separately. This is defined outside of region I of parameter space and is independent of length of chain N. We can see the expected $h = 1$ and $\gamma = 0$ transitions clearly.

already calculated.

$$\tilde{g}_{\gamma\gamma} = -\frac{1}{N}\sum_{k,k\neq k^*}\left(\frac{\partial\theta_k}{\partial\gamma}\right)^2, \tag{3.23}$$

$$= -\frac{1}{2}\frac{1}{4\pi}\int_0^\pi dk\left\{\frac{c(1+\gamma^2)+\cos k}{[c(1-\gamma^2)+\cos k]^2+\gamma^2\sin^2 k}\right\}^2\sin^2 k + \frac{1}{N}\left(\frac{\partial\theta_*}{\partial\gamma}\right)^2 \tag{3.24}$$

While the k^* term can be calculated by straight forward derivation, the integral is a bit more complicated and can be calculated through contour integration in the complex plane. See Appendix C.4 for more details on that. The fidelity susceptibility along the parabolas in region I is

$$\tilde{g}_{\gamma\gamma} = -\frac{1}{16}\frac{1+c^2(1+\gamma)^3(3\gamma-1)}{\gamma[1+\gamma)^2(1-c^2(1-\gamma^2)^2]} + \frac{1}{4N}\frac{c^2(1-c^2)}{[1-c^2(1-\gamma^2)]^2}. \tag{3.25}$$

Since we are moving along parabolas, we expect to see only the $\gamma = 0$ transition, and that is exactly what happens, even for smaller N. This is an excellent example of how the susceptibility is a "cleaner" measure. However, one could argue that it is still effectively an intensive quality as the $1/N$ correction is so small it does not affect the curve.

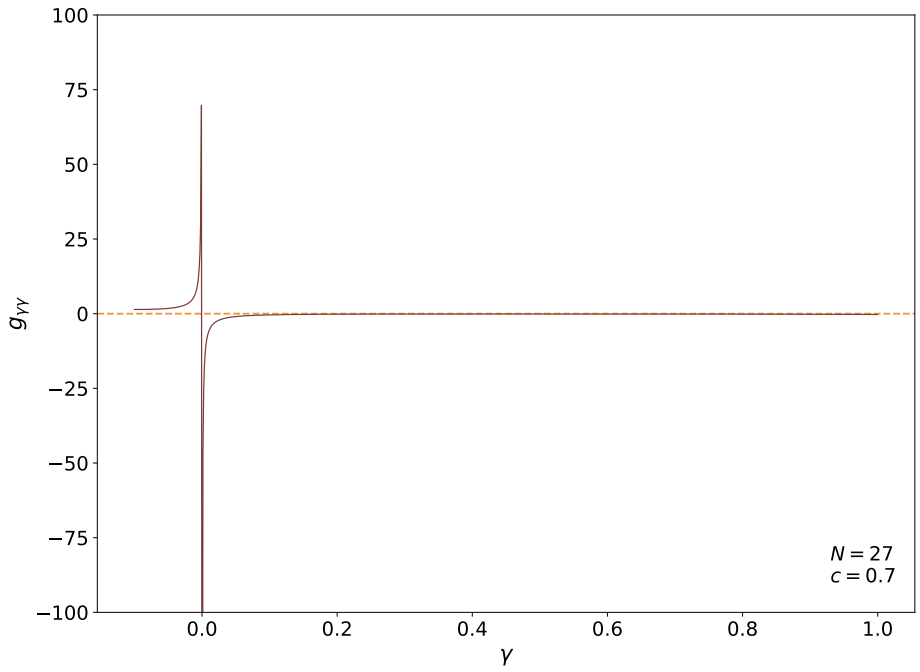

Figure 3.8: Fidelity susceptibility in the case of antiferromagnetic order $J = +1$ along a chosen parabola $c = 0.7$ in range $\gamma = [-0.1, 1.0]$. We see a clean discontinuity at $\gamma = 0$ as expected.

Although we did obtain an analytical expression for susceptibility in the most problematic region I, alas only along each parabola respectively. The inability to define it moving in any direction differing from the parabolas renders further attempt at criticality analysis in this way futile. That is why we proceed with a slightly altered version of fidelity, called reduced fidelity.

3.2 Reduced fidelity

We have shown in Section 3.1 that global fidelity and its susceptibility, albeit convenient for analysis in "normal" circumstances, which involve every part of the ferromagnetic and antiferromagnetic parameter space except for the area bounded by the parabola $h < 1 - \gamma^2$, is unfit to describe and even undefinable in the aforementioned region I. Furthermore, looking to future experimental realizations, it is advisable to look for more adequate quantities whose measurements will be more feasible and attainable.

Both of these arguments can be fulfilled in reduced fidelity, an alternative method

that has been proposed and applied to models with continuous level-crossings, like the Heisenberg chain. [17, 18]. It is based on taking reduced density matrices of the system, thereby examining a subsystem instead of the whole system

$$\mathcal{F}^R = \mathrm{Tr}\,\sqrt{\rho^{1/2}\tilde{\rho}\rho^{1/2}}, \tag{3.26}$$

where the notation follows from before, with ρ denoting the reduced density matrix of the ground state (h, γ), and $\tilde{\rho} = \rho(h + dh, \gamma + d\gamma)$. The idea behind this approach is that although the ground state of the full system is represented by a pure state, the ground state of the reduced system is instead generally described by a mixed state, thereby reducing the degree of orthogonality and allowing for deeper analysis.

We opted for a two-site reduced density matrix, which can be expressed using two-point correlation functions as follows [23]

$$\rho_{ij} = \sum_{\alpha,\beta=0}^{3} \langle \sigma_i^\alpha \sigma_j^\beta \rangle \; \sigma_i^\alpha \otimes \sigma_j^\beta, \tag{3.27}$$

where σ^0 denotes the 2×2 identity matrix, and indices $1-3$ stand for x, y, z. Because of symmetries, most of the coefficients $\langle \sigma_i^\alpha \sigma_j^\beta \rangle$ vanish. For example, reflection symmetry around any site implies $\rho_{ij} = \rho_{ji}$. The Hamiltonian being real means $\rho_{ij}^* = \rho_{ij}$. Furthermore, the system preserves parity (2.12).

The calculations for obtaining the one and two-point correlators in the ground state are rather involved. We're interested in $\langle \sigma_i^\alpha \sigma_j^\beta \rangle$, but the only expectation we know is for the Bogoliubov fermions $\langle \chi_q \chi_{q'}^{(\dagger)} \rangle$. We will need to use all the transformations we used to solve the XY chain and go backwards through them to connect the sought after correlator, and the one we know.

3.2.1 Correlation functions

We start by expressing the "regular" Pauli matrices σ_i^α, that is, their two-point correlation functions over the lowering and raising operators. Of course, the σ_i^z operator stays the same and we only transform the σ_i^x and σ_i^y operators. Using (2.3) and the aforementioned symmetries of the system, we prove that the mixed correlators vanish and all that is left are the $\langle \sigma_i^\alpha \sigma_j^\alpha \rangle$ functions, along with one-point functions $\langle \sigma_i^z \rangle$.

$$\langle \sigma_i^{x,y} \sigma_j^{x,y} \rangle = \pm \langle \sigma_i^+ \sigma_j^+ \pm \sigma_i^+ \sigma_j^- \pm \sigma_i^- \sigma_j^+ + \sigma_i^- \sigma_j^- \rangle, \tag{3.28a}$$

$$\langle \sigma_i^x \sigma_j^y \rangle = \langle \sigma_i^x \sigma_j^z \rangle = \langle \sigma_i^y \sigma_j^z \rangle = 0. \tag{3.28b}$$

Finally expanding (3.27), in the basis $\{|\uparrow\uparrow\rangle, |\uparrow\downarrow\rangle, |\downarrow\uparrow\rangle, |\downarrow\downarrow\rangle\}$,the reduced density matrix takes the form

$$\rho_{ij} = \frac{1}{4} \begin{pmatrix} a^+ & 0 & 0 & c^- \\ 0 & b & c^+ & 0 \\ 0 & c^+ & b & 0 \\ c^- & 0 & 0 & a^- \end{pmatrix}, \tag{3.29}$$

with

$$a^\pm = 1 \pm \langle \sigma_i^z \rangle \pm \langle \sigma_j^z \rangle + \langle \sigma_i^z \sigma_j^z \rangle, \tag{3.30a}$$

$$b = 1 - \langle \sigma_i^z \sigma_j^z \rangle, \tag{3.30b}$$

$$c^\pm = \langle \sigma_i^x \sigma_j^x \rangle \pm \langle \sigma_i^y \sigma_j^y \rangle. \tag{3.30c}$$

The next step is relating these $\sigma^{\pm,z}$ operators to fermions, i.e., again doing a Jordan-Wigner transformation (2.7). While doing that, we will introduce a new pair of operators which are standard in this procedure, and which will, surprisingly, help us declutter the notation.

If we start transforming, for example, $\langle \sigma_i^x \sigma_j^x \rangle$ into the Jordan-Wigner fermions we will have

$$\langle \sigma_i^x \sigma_j^x \rangle = \Big\langle \prod_{l=j}^{i-1} (1 - 2\psi_l^\dagger \psi_l)(\psi_i + \psi_i^\dagger)(\psi_j + \psi_j^\dagger) \Big\rangle. \tag{3.31}$$

Now we define the new operators A_i and B_i

$$A_i \equiv \psi_i^\dagger + \psi_i, \quad B_i \equiv \psi_i^\dagger - \psi_i, \tag{3.32}$$

which, with a little manipulation (see Appendix (D.1)), allow us to write:

$$= \Big\langle \prod_{l=j}^{i-1} A_l B_l A_i A_j \Big\rangle = \Big\langle \prod_{l=j+1}^{i-1} A_j A_j B_j A_l B_l A_i \Big\rangle \tag{3.33}$$

$$= \Big\langle \prod_{l=j+1}^{i-1} B_j A_l B_l A_i \Big\rangle. \tag{3.34}$$

Similarly, we obtain the other two correlators. Writing them all in one place we have

$$\langle \sigma_i^x \sigma_j^x \rangle = \big\langle B_j A_{j+1} B_{j+1} A_{j+2} B_{j+2} \cdot \cdots \cdot A_{i-1} B_{i-1} A_i \big\rangle, \tag{3.35a}$$

$$\langle \sigma_i^y \sigma_j^y \rangle = \big\langle B_{j+1} A_j B_{j+2} A_{j+1} \cdot \cdots \cdot B_i A_{i-1} \big\rangle, \tag{3.35b}$$

$$\langle \sigma_i^z \sigma_j^z \rangle = \big\langle A_i B_i A_j B_j \big\rangle. \tag{3.35c}$$

Luckily, we can turn this result back to two-point correlators by using Wick's theorem [24]. Wick's theorem states that if we have a linear combination of fermionic operators (which A_i and B_i are), the expectation of a product of an even number of those operators in the vacuum state can be decomposed into a sum over all distinct combinations of two-point expectations multiplied by a permutation sign factor. If the product is of an odd number of operators, it is immediately zero.
We proceed with using Wick's theorem on the correlators, choosing pairings of $\langle B_k A_l \rangle$ and fixing the sign to permutations of A. The correlation functions are now

$$\langle \sigma_i^x \sigma_j^x \rangle = \sum_p (-1)^p \big\langle B_j A_{P(j+1)} \big\rangle \big\langle B_{j+1} A_{P(j+2)} \big\rangle \cdot \cdots \cdot \big\langle B_{i-1} A_{P(i)} \big\rangle, \tag{3.36a}$$

$$\langle \sigma_i^y \sigma_j^y \rangle = \sum_p (-1)^p \big\langle B_{j+1} A_{P(j)} \big\rangle \big\langle B_{j+2} A_{P(j+1)} \big\rangle \cdot \cdots \cdot \big\langle B_i A_{P(i-1)} \big\rangle, \tag{3.36b}$$

$$\langle \sigma_i^z \sigma_j^z \rangle = \big\langle B_i A_i \big\rangle \big\langle B_j A_j \big\rangle - \big\langle B_i A_j \big\rangle \big\langle B_i A_j \big\rangle. \tag{3.36c}$$

One can notice there are missing $\big\langle A_i A_j \big\rangle$ and $\big\langle B_i B_j \big\rangle$ correlators. That is because they vanish, as is shown in Appendix D.1.

Turns out, this expression coincides with the Leibniz formula for the determinant of a matrix. The two-site x correlation function written as a matrix determinant is

then

$$\langle \sigma_i^x \sigma_j^x \rangle = \begin{vmatrix} \langle B_j A_{j+1} \rangle & \langle B_j A_{j+2} \rangle & \cdots & \langle B_j A_i \rangle \\ \langle B_{j+1} A_{j+1} \rangle & \langle B_{j+1} A_{j+2} \rangle & \cdots & \langle B_{j+1} A_i \rangle \\ \vdots & \vdots & \ddots & \vdots \\ \langle B_{i-1} A_{j+1} \rangle & \langle B_{i-1} A_{j+2} \rangle & \cdots & \langle B_{i-1} A_i \rangle \end{vmatrix}. \tag{3.37}$$

The expression for $\langle \sigma_i^y \sigma_j^y \rangle$ is similar

$$\langle \sigma_i^y \sigma_j^y \rangle = \begin{vmatrix} \langle B_{j+1} A_j \rangle & \langle B_{j+1} A_{j+1} \rangle & \cdots & \langle B_{j+1} A_{i-1} \rangle \\ \langle B_{j+2} A_j \rangle & \langle B_{j+2} A_{j+1} \rangle & \cdots & \langle B_{j+2} A_{i-1} \rangle \\ \vdots & \vdots & \ddots & \vdots \\ \langle B_i A_j \rangle & \langle B_i A_{j+2} \rangle & \cdots & \langle B_i A_{i-1} \rangle \end{vmatrix}. \tag{3.38}$$

Interestingly, the z correlator can also be written as a matrix determinant

$$\langle \sigma_i^z \sigma_j^z \rangle = \begin{vmatrix} \langle B_i A_i \rangle & \langle B_i A_j \rangle \\ \langle B_i A_j \rangle & \langle B_j A_j \rangle \end{vmatrix}. \tag{3.39}$$

Right now, we have a connection between operators A and B and the Jordan-Wigner real-space fermions ψ_i. The next and final stage comprises of finding the expectation of the Fourier-space fermions ψ_q and linking that to real-space fermions through (2.20). The link between the real and Fourier space is given in the following expressions

$$\langle \psi_i \psi_j \rangle = \frac{i}{N} \sum_{k,q} e^{i\frac{2\pi}{N}(ki+qj)} \langle \psi_k \psi_q \rangle, \tag{3.40a}$$

$$\langle \psi_i^\dagger \psi_j^\dagger \rangle = \frac{-i}{N} \sum_{k,q} e^{-i\frac{2\pi}{N}(ki+qj)} \langle \psi_k^\dagger \psi_q^\dagger \rangle, \tag{3.40b}$$

$$\langle \psi_i \psi_j^\dagger \rangle = \frac{1}{N} \sum_{k,q} e^{i\frac{2\pi}{N}(ki-qj)} \langle \psi_k \psi_q^\dagger \rangle, \tag{3.40c}$$

$$\langle \psi_i^\dagger \psi_j \rangle = \frac{1}{N} \sum_{k,q} e^{-i\frac{2\pi}{N}(ki-qj)} \langle \psi_k^\dagger \psi_q \rangle. \tag{3.40d}$$

Proceeding to the expectation of Fourier-space fermions, we have at last reached the final transformation and the Bogoliubov fermion. This is where we consider which ground state are we using. By reasoning mentioned before in Section 2.2.2, we will consider only the even sector ground state. Up to this point the derivation

has been completely general. Now we will choose to calculate the correlations in the area outside of region I where the ground state is the vacuum, taking special care of the differences occurring in the case of frustrated vacuum which is region II'. After completion, we will repeat the process for the double-degenerate, double-excited ground state of region I.

Vacuum ground state We use (2.34), (2.33) and (2.42) to obtain the following result

$$\langle \psi_k \psi_q \rangle = -\cos\theta_k \sin\theta_q \delta_{k,-q}, \tag{3.41a}$$

$$\langle \psi_k^\dagger \psi_q^\dagger \rangle = -\sin\theta_k \cos\theta_q \delta_{-k,q}, \tag{3.41b}$$

$$\langle \psi_k \psi_q^\dagger \rangle = \cos\theta_k \cos\theta_q \delta_{k,q}, \tag{3.41c}$$

$$\langle \psi_k^\dagger \psi_q \rangle = \sin\theta_k \sin\theta_q \delta_{-k,-q}. \tag{3.41d}$$

Finally, we combine this result with (3.40). To link that to the A_i and B_i correlators, we have to do an another little reverse-transformation after all- writing A_i and B_i again as real-space fermions.

$$\langle A_i B_i \rangle = \langle 1 - 2\psi_i^\dagger \psi_i \rangle = 1 - \frac{2}{N} \sum_q \sin^2\theta_q, \tag{3.42a}$$

$$\begin{aligned} \langle A_i B_j \rangle &= \langle (\psi_i^\dagger + \psi_i)(\psi_j^\dagger - \psi_j) \rangle \\ &= -\frac{1}{N} \sum_q \left\{ \sin 2\theta_q \sin\left[\frac{2\pi}{N} q(i-j)\right] + \cos 2\theta_q \cos\left[\frac{2\pi}{N} q(i-j)\right] \right\}, \end{aligned} \tag{3.42b}$$

$$\langle B_i A_j \rangle = -\langle A_j B_i \rangle = \frac{1}{N} \sum_q \left\{ -\sin 2\theta_q \sin\left[\frac{2\pi}{N} q(i-j)\right] + \cos 2\theta_q \cos\left[\frac{2\pi}{N} q(i-j)\right] \right\}. \tag{3.42c}$$

In the last two equations we have used the fact we are summing, or in the thermodynamic limit integrating, over the whole Brillouin zone and therefore we can discard the odd (even) part of the exponential if multiplied by an even (odd) function.

Lastly, a quick calculation of the one-point function σ_i^z, i.e. the magnetisation along z, provides us with

$$\langle \sigma_i^z \rangle = 1 - 2\psi_i^\dagger \psi_i = \langle A_i B_i \rangle \tag{3.43}$$

Now that we have the elements of the matrices both, it is time to obtain the full expression. Whilst expanding the θ_q in (3.42a), one should keep in mind that $\theta_\pi = 0$ which interferes with using (A.3b). While $\sin 2\theta_\pi$ is correctly zero, it is not enough to simply take $k = \pi$ because for $h < 1$ we obtain $\cos 2\theta_\pi = -1$. That is why it in region II' we need to separate it from the sum

$$\begin{aligned}
\big\langle A_i B_j \big\rangle_{II'} =& -\frac{1}{N}\sum_q \left\{ \sin 2\theta_q \sin\left[\frac{2\pi}{N} q(i-j)\right] + \cos 2\theta_q \cos\left[\frac{2\pi}{N} q(i-j)\right] \right\} && (3.44)\\
=& -\frac{1}{N}\sum_{q\neq N/2} \left\{ \sin 2\theta_q \sin\left[\frac{2\pi}{N} q(i-j)\right] + \cos 2\theta_q \cos\left[\frac{2\pi}{N} q(i-j)\right] \right\} && (3.45)\\
& -\frac{1}{N}\cos\left[\frac{2\pi}{N} q(i-j)\right]. && (3.46)
\end{aligned}$$

Now, we can complete the sum by adding and subtracting the term corresponding to the "wrong" definition of $\cos 2\theta_\pi$

$$\begin{aligned}
=& -\frac{1}{N}\sum_q \left\{ \sin 2\theta_q \sin\left[\frac{2\pi}{N} q(i-j)\right] + \cos 2\theta_q \cos\left[\frac{2\pi}{N} q(i-j)\right] \right\} && (3.47)\\
& -\frac{1}{N}\cos\left[\frac{2\pi}{N} q(i-j)\right] + \frac{h-1}{\Lambda_\pi}\cos\left[\frac{2\pi}{N} q(i-j)\right] && (3.48)\\
\big\langle A_i B_j \big\rangle_{II'} =& -\frac{1}{N}\sum_q \left\{ \sin 2\theta_q \sin\left[\frac{2\pi}{N} q(i-j)\right] + \cos 2\theta_q \cos\left[\frac{2\pi}{N} q(i-j)\right] \right\} && (3.49)\\
& -\frac{2}{N}\cos\left[\frac{2\pi}{N} q(i-j)\right]. && (3.50)
\end{aligned}$$

It is worth noticing that the correlator (3.42a) depends only on the difference $i-j$ and not i, j themselves. That greatly simplifies the matrices (3.37) and (3.38). If we introduce a function $g(r)$ as a shorthand

$$g(r) = g(i-j) = \big\langle B_i A_j \big\rangle. \tag{3.51}$$

The matrices are then given by

$$\langle \sigma_i^y \sigma_j^y \rangle = \begin{vmatrix} g(-1) & g(0) & \cdots & g(-r) \\ g(0) & g(1) & \cdots & g(r-1) \\ \vdots & \vdots & \ddots & \vdots \\ g(r-2) & g(r-3) & \cdots & g(-1) \end{vmatrix}. \tag{3.52}$$

$$\langle \sigma_i^y \sigma_j^y \rangle = \begin{vmatrix} g(1) & g(0) & \cdots & g(-r-2) \\ g(2) & g(1) & \cdots & g(-r-1) \\ \vdots & \vdots & \ddots & \vdots \\ g(r) & g(r-1) & \cdots & g(1) \end{vmatrix}. \tag{3.53}$$

Region I Now that we have the correlation functions for the vacuum state, we need to calculate them for the frustrated, double-degenerate, double-excited state of region I (2.63). The computations follow naturally from the vacuum scenario and are straight forward, yet they are considerably more tedious.

For each expectation we also need to separately consider the scenario $q, k = \pi$ because of (2.36). Luckily, since the ground state already has a π excitation, when only one moment is π we can always achieve $\chi_{pi}^2 = 0$. When both momenta are π it is also very simple since we either have $\psi_{pi}^2 = 0$ right from the start, or we can use (2.36) and have $\langle \chi \pi^\dagger \chi \pi \rangle = 0$, whereas by (2.37) $\langle \chi \pi \chi \pi^\dagger \rangle = 1$.
As for the rest of the momenta, we had to use (2.37) excessively to manipulate the 16 terms per each expectation. Therefore, here we will only present the results. For more details, see Appendix D.2.

$$\langle \psi_k \psi_q \rangle = \frac{1}{2} \sin 2\theta_q \, \delta_{k,-q}(1 - \delta_{q,k*} - \delta_{q,-k*}), \tag{3.54a}$$

$$\langle \psi_k^\dagger \psi_q^\dagger \rangle = \frac{1}{2} \sin 2\theta_q \, \delta_{-k,q}(\delta_{q,k*} + \delta_{q,-k*} - 1), \tag{3.54b}$$

$$\langle \psi_k \psi_q^\dagger \rangle = -\frac{1}{2}\delta_{k,-q}(\delta_{q,k*} + \delta_{q,-k*}) + \frac{1}{2}\delta_{k,q}[2\sin^2\theta_q + (\delta_{q,k*} + \delta_{q,-k*})\cos 2\theta_q], \tag{3.54c}$$

$$\langle \psi_k^\dagger \psi_q \rangle = \delta_{k,q} + \frac{1}{2}\delta_{k,-q}(\delta_{q,k*} + \delta_{q,-k*}) - \frac{1}{2}\delta_{k,q}[2\sin^2\theta_q + (\delta_{q,k*} + \delta_{q,-k*})\cos 2\theta_q]. \tag{3.54d}$$

Combining these with the same expressions for expectations of $\langle A_i B_j \rangle$ as in the vacuum scenario 3.2.1, we obtain

$$\langle A_i B_i \rangle = \langle A_i B_i \rangle_{\text{vac}} + \frac{2}{N}\left(\cos\frac{4\pi}{N}k^* i - \cos 2\theta_*\right), \tag{3.55a}$$

$$\langle A_i B_j \rangle = \langle A_i B_j \rangle_{\text{vac}} + \frac{2}{N}\left[\sin 2\theta_* \sin(i-j)k^* - \cos 2\theta_* \cos(i-j)k^* + \cos(i+j)k^*\right]. \tag{3.55b}$$

In region I we again have $h < 1$ and therefore obtain the π correction derived for

region II'.

Summing up, the correlation functions for the even sector ground states are given by

$$\langle A_i B_j \rangle = \langle A_i B_j \rangle_0 + C^{(1)} + C^{(2)}(h,\gamma), \tag{3.56}$$

where we have dubbed the "normal" vacuum sum (with π included) with index 0 and defined functions $C^{(1)}$ and $C^{(2)}_{i,j}(h,\gamma)$ which contain the necessary corrections.

$$C^{(1)} = \begin{cases} -\frac{2}{N}\cos\left[\frac{2\pi}{N}q(i-j)\right], & h<1 \\ 0, h>1 \end{cases} \tag{3.57}$$

$$C^{(2)}(h,\gamma) = \begin{cases} \frac{2}{N}\left(\cos\frac{4\pi}{N}k^* i - \cos 2\theta_*\right), & i=j,\ h<1-\gamma^2 \\ \frac{2}{N}\left[\sin 2\theta_* \sin(i-j)k^* - \cos 2\theta_* \cos(i-j)k^* + \cos(i+j)k^*\right], & i\neq j,\ h<1-\gamma^2 \\ 0, & h>1-\gamma^2 \end{cases} \tag{3.58}$$

Combining with (3.37), (3.38), (3.39) and (5.36), we have effectively calculated the correlation functions for the vacuum. This concludes calculating the correlation functions of the system. We proceed with analysing reduced fidelity and its susceptibility.

3.2.2 Results

We study the two-point reduced fidelity for next neighbours spins which is displayed in Figure 3.9. We observe oscillatory behaviour for small enough N. This comes from the correction in the frustrated region (3.57), (3.58) which produces peaks associated with k^* but through trigonometric functions which induce oscillations. These oscillations soon vanish with increasing N, as can be seen in the smaller graph in Figure 3.9.

Nonetheless, there is one dominant peak which perseveres even when the oscillations die out. That peak corresponds to the final parabola $c=1$, that is, the edge of region I and we will refer to it as the π-peak. It seems as if it could be a signature of a phase transition between the frustrated region I and the rest. However, it also

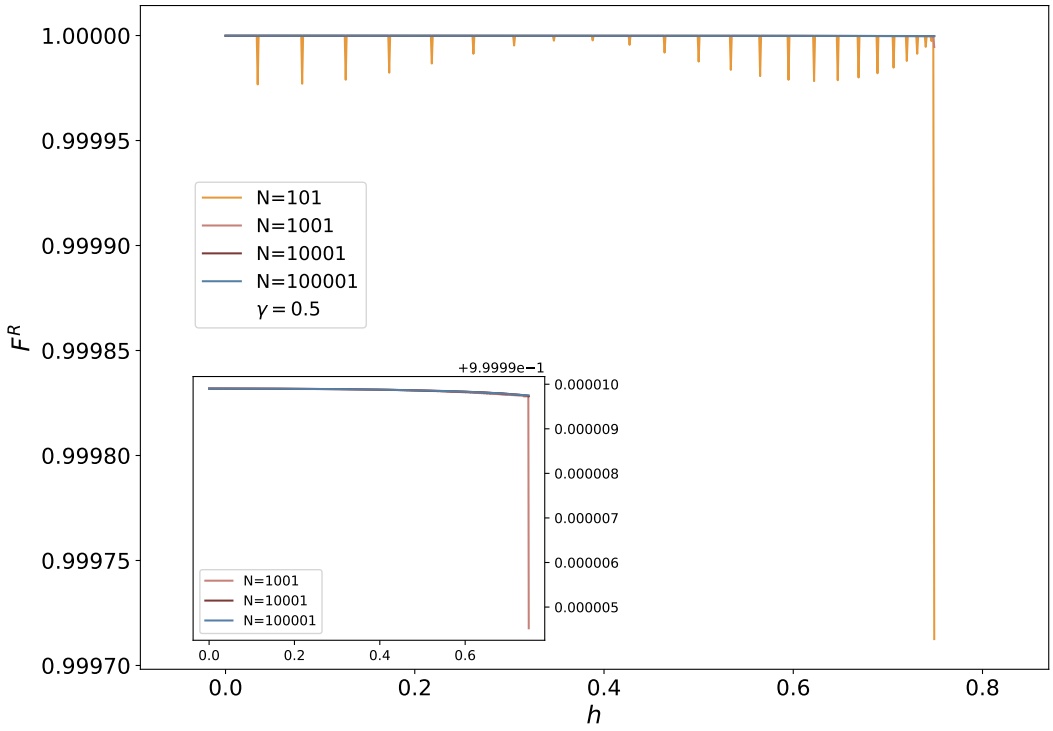

Figure 3.9: Reduced fidelity in the case of antiferromagnetic order $J = +1$ for next-neighbours $r = 1$ with fixed anisotropy $\gamma = 0.5$ in region I $h = [0.1, 0.75]$. The smaller graph is there to show the oscillations vanish already after the first increase by an order of magnitude of N.

decreases with increasing N, albeit more slowly. That is why we check the amplitude of the π-peak for N in increasing orders of magnitude in Figure 3.10.

It seems that even the π-peak disappears in the thermodynamic limit. What's more, it decreases essentially with $\frac{1}{N^2}$. There is hope that maybe, instead of looking at next-neighbours spins, taking an extensive distance in sites (r), for example antipodal sites $r = \frac{N-1}{2}$ can offset the decrease and the π-peak might saturate into some finite value. Unfortunately, Figure 3.11 is not the case.

Not only that the π-peak also decreases and vanishes in the thermodynamic limit, but the exponent by which it decreases is, in effect, the same as for next neighbours $\frac{1}{N^2}$.

In conclusion, unfortunately for experimental realizations, the two-point reduced fidelity is able to capture all of the critical points only for finite size chains. In the thermodynamic limit it loses characteristics imposed by frustration.

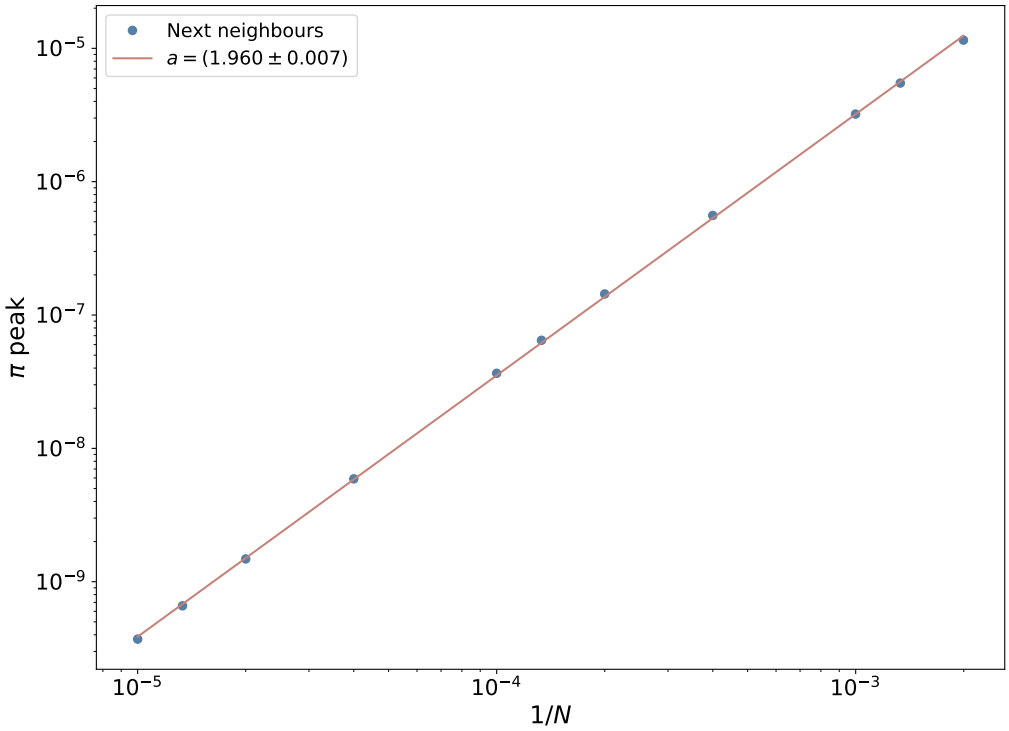

Figure 3.10: The amplitude of the π-peak for next-neighbours $r = 1$ with fixed anisotropy $\gamma = 0.5$ in region I $h = [0.1, 0.75]$. The amplitude decreases by N^{-a}.

3.2.3 Reduced fidelity susceptibility

To be able to obtain an analytical expression for the reduced fidelity susceptibility it is necessary to rearrange the basis into $\{|\uparrow\uparrow\rangle, |\downarrow\downarrow\rangle, |\uparrow\downarrow\rangle, |\downarrow\uparrow\rangle\}$, turning (5.36) into a block-diagonal matrix

$$\rho_{ij} = \frac{1}{4}\begin{pmatrix} a^+ & c^- & 0 & 0 \\ c^- & a^- & 0 & 0 \\ 0 & 0 & b+d & c^+ \\ 0 & 0 & c^+ & b-d \end{pmatrix} = \bigoplus_{l=1}^{2} \rho_l, \tag{3.59}$$

with

$$d = \langle \sigma_i^z \rangle - \langle \sigma_j^z \rangle. \tag{3.60}$$

Then, the reduced fidelity susceptibility, assuming $\mathrm{Tr}\,\rho_l \neq 0$ and $\det \rho_l \neq 0$, is [18]

$$\chi_\lambda = \chi_{1,\lambda} + \chi_{2,\lambda}, \tag{3.61}$$

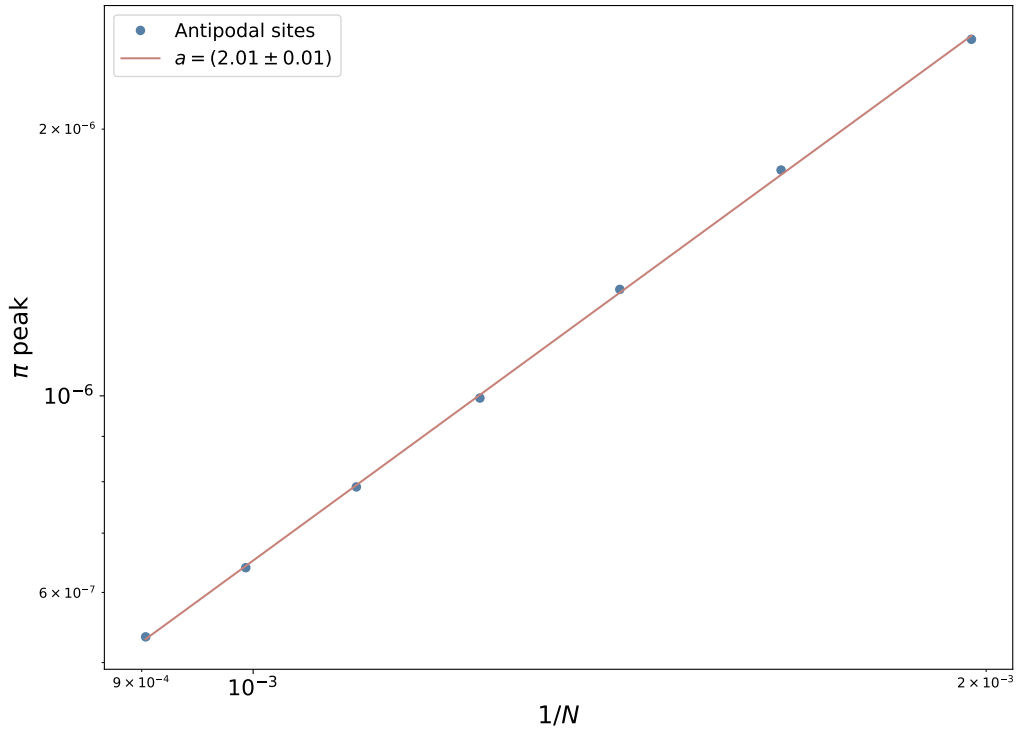

Figure 3.11: The amplitude of the π-peak for extensive distance $r = \frac{N-1}{2}$ with fixed anisotropy $\gamma = 0.5$ in region I $h = [0.1, 0.75]$. The amplitude decreases by N^{-a}.

where

$$\chi_{l,\lambda} = \frac{1}{4\,\mathrm{Tr}\,\rho_l}\left\{\left[\mathrm{Tr}\,\partial_\lambda\rho_l\right]^2 - 4\det(\partial_\lambda\rho_l) + \frac{[\partial_\lambda \det(\rho_l)]^2}{\det(\rho_l)}\right\}. \tag{3.62}$$

Using numerical calculations, we were able to plot (3.61). The result is shown in 3.12 and it follows the expectations acquired in Figure 3.9. Oscillations for small N are again present, and they again die out for large enough N. By studying the π in 3.13, we again obtain an exponent of around 2, implying a $1/N^2$ decrease.

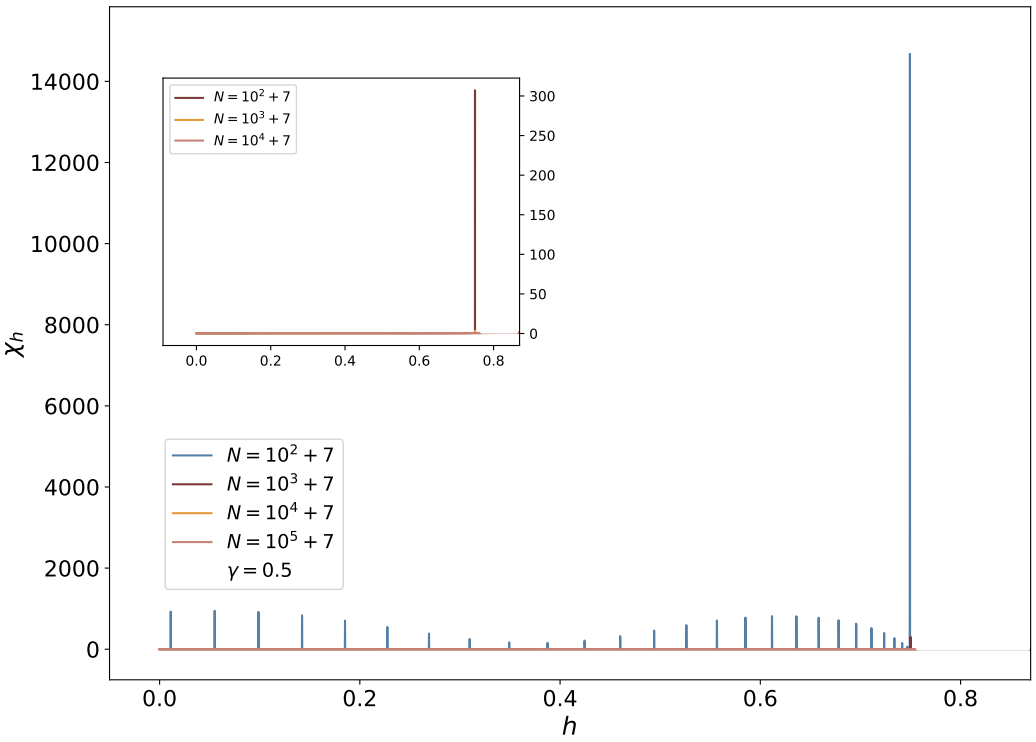

Figure 3.12: Reduced fidelity susceptibility for $\gamma = 0.5$ and nearest neighbours in the case of antiferromagnetic ordering $J = 1$.

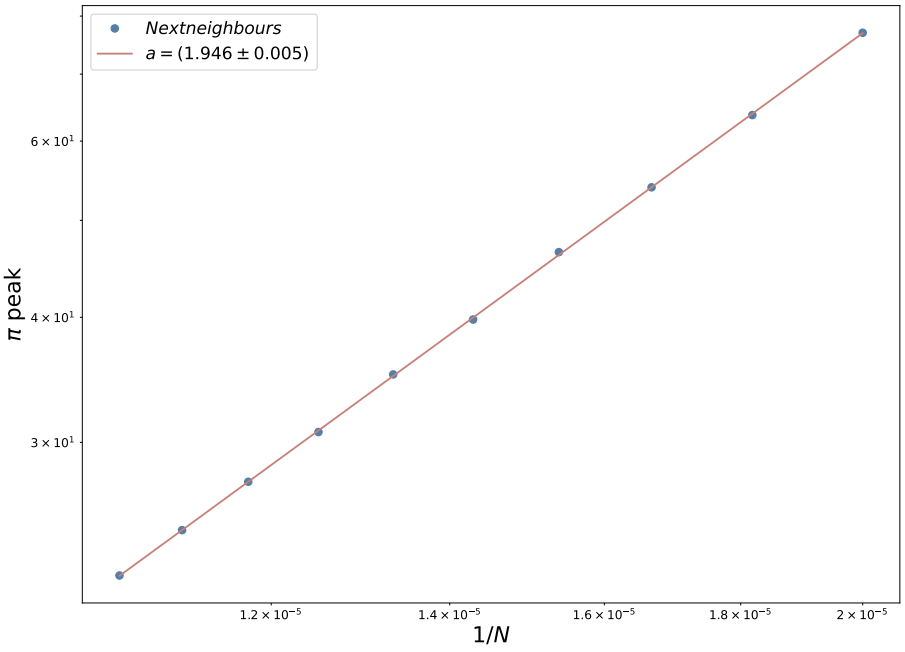

Figure 3.13: The amplitude of the π-peak for extensive distance $r = \frac{N-1}{2}$ with fixed anisotropy $\gamma = 0.5$ in region I $h = [0.1, 0.75]$. The amplitude decreases by N^{-a}.

4 Conclusion

The aim of this thesis was to study the effects of frustration on the geometrical properties of the ground state by comparison between the frustrated and unfrustrated spin chain. We have chosen the one dimensional XY model for this purpose.

We began by examining the XY model and solving it analytically by mapping the spin system to a free fermion system (Jordan-Wigner transformation), moving into Fourier space and finally arriving at a diagonal Hamiltonian by a Bogoliubov rotation. We classified the ground state in great detail, looking at both the ferromagnetic and antiferromagnetic ordering, as well as even and odd number of spins, dividing the parameter space into regions with different properties. We observed that in the case of frustrated boundary conditions, i.e. antiferromagnetic periodic chains with an odd number of spins, for $h < 1$ the system is frustrated and displays that through favoring excited states as its ground state. One such excitation is especially intriguing as it changes with the variation of parameters, thereby inducing level-crossings which in the thermodynamic limit become continuous.

After setting up the model, we turned to the main objective of the thesis which was analyzing the ground state geometry by calculating the fidelity and its susceptibility between ground states with slightly varied parameters h and γ. Fidelity, an overlap function is assumed to be able to construct the phase diagram of the given system by exhibiting a sudden drop at the critical point. Calculating the overlap for the different ground states of the system, we obtained the expression which was very similar across regions but still managed to produce all the expected behaviour. The well known phase transitions $h = 1$ and $\gamma = 0$ were retrieved by the fidelity approach. However, we have found the fidelity drop to exact zero for the level-crossings induced by the changing excitation momenta in the frustrated region, making susceptibility undefinable except if moving along special curves in the parameter space.

These continuous level-crossings led us to look at a smaller subsystem by calculating the reduced fidelity, which is based on reduced density matrices. To do so we calculated the two-point correlators by moving through the mentioned transformations back and forth. What we discovered was that the almost continuous level-crossings which should, by widely-accepted assumption, signal the existence of a phase transition vanished in the thermodynamic limit and thereby did not constitute as phase

transitions. We have found a counter example for the well accepted notion that fidelity approach can be used to characterise systems without any *a priori* knowledge of the system.

Appendices

Appendix A Solution details

A.1 Fourier transform operators

If we notice that

$$\begin{aligned} x_0 \in \mathbb{Z} \Rightarrow \frac{1}{N}\sum_{x\in X_N} e^{i\frac{2\pi}{N}xn} &= \begin{cases} 1, & n = kN, k \in \mathbb{Z} \\ 0, & \text{else} \end{cases} \\ x_0 = \tfrac{1}{2} \Rightarrow \frac{1}{N}\sum_{x\in X_N} e^{i\frac{2\pi}{N}xn} &= \begin{cases} (-1)^k, & n = kN, k \in \mathbb{Z} \\ 0, & \text{else} \end{cases} \end{aligned} \tag{A.1}$$

then we can write the operator ψ_j for all $j = 1, .., N$ like

$$\psi_j = \sum_{l=1}^{N} \left[\psi_l \frac{1}{N} \sum_{x\in X_N} e^{\frac{2\pi}{N}x(j-l)} \right]. \tag{A.2}$$

It is not important what we take for x_0, an integer or $1/2$. However, by choosing $x_0 = 1/2$ in the even sector and $x_0 = 0$ in the odd sector, we're able to continue with periodic boundary conditions and define ψ_{N+1} in line with (A.2). Now we see why it's convenient to define operators ψ_q like (2.17) and why we call them Fourier transform of ψ_j.

A.2 Trigonometric properties

It is sometimes convenient to rearrange equations (2.29) into a different form

$$\tan 2\theta_q = \frac{J\gamma \sin\left(\frac{2\pi}{N}q\right)}{h + J\cos\left(\frac{2\pi}{N}q\right)}, \tag{A.3a}$$

$$e^{i2\theta_q} = \frac{h + J\cos\left(\frac{2\pi}{N}q\right) + iJ\gamma\sin\left(\frac{2\pi}{N}q\right)}{\sqrt{\left[h + J\cos\left(\frac{2\pi}{N}q\right)\right]^2 + J^2\gamma^2\sin^2\left(\frac{2\pi}{N}q\right)}}. \tag{A.3b}$$

Appendix B Ground state

To obtain the correct form for the ground state of the quantum XY chain, we start by expanding (2.41) by the commutation relation for χ_q (2.37b).

$$
\begin{aligned}
&1 \cdot \psi_q \left|0\right\rangle = 0, \\
&\chi_q \chi_q^\dagger + \chi_q^\dagger \chi_q) \psi_q \left|0\right\rangle = 0, \\
&(\cos\theta_q \psi_q - \sin\theta_q \psi_{-q}^\dagger)(\cos\theta_q \psi_q^\dagger - \sin\theta_q \psi_{-q}) \psi_q + \\
&(\cos\theta_q \psi_q^\dagger - \sin\theta_q \psi_{-q})(\cos\theta_q \psi_q - \sin\theta_q \psi_{-q}^\dagger) \psi_q = 0.
\end{aligned}
$$

Further expansion and manipulation is done by using (2.18)

$$
\begin{aligned}
&\psi_q^\dagger \psi_q = 1 - \psi_q \psi_q^\dagger, \qquad (\psi_q)^2 = (\psi_q^\dagger)^2 = 0. \\
&(\chi_q \cos\theta_q + cos\theta_q \psi_q \cdot \sin\theta_q \psi_q^\dagger \psi_{-q}^\dagger + \sin^2\theta_q \psi_{-q}^\dagger \psi_{-q}^\dagger \psi_q^\dagger) \left|0\right\rangle = 0,
\end{aligned}
$$

where it was possible to add the last term because it is 0

$$
\psi_{-q}^\dagger \psi_{-q}^\dagger = 0 \quad \Rightarrow \quad \sin^2\theta_q \psi_{-q}^\dagger \psi_{-q}^\dagger \psi_q^\dagger = 0.
$$

Finally, we obtain the desired term

$$
\chi_q(\cos\theta_q + \sin\theta_q \, \psi_q^\dagger \psi_{-q}^\dagger) \left|0\right\rangle = 0.
$$

Appendix C Global fidelity

C.1 One excitation fidelity

When we calculate the fidelity (3.7), what is important is that we have four different combinations of ψ_Q fermion pairs. For example, in the calculation there is the following term

$$\langle vac|\, \cos\theta_q \cos\tilde{\theta}_q\, \psi_Q\, \psi_Q^\dagger \bigotimes_{q=0}^{\left\lfloor \frac{N-1}{2} \right\rfloor} \left(\cos\theta_q \left|0\right\rangle_q \left|0\right\rangle_{-q} + \sin\theta_q \left|1\right\rangle_q \left|1\right\rangle_{-q} \right) \tag{C.1}$$

The $\psi_Q\, \psi_Q^\dagger$ operators act as per (2.9) and only on the $q = Q$ term from the product, finally resulting in a factor of $\cos^2\theta_q \cos^2\tilde{\theta}_Q$. This is multiplied by the rest of the product for which there is only the vacuum (and therefore the result of the vacuum fidelity). Doing the same for the rest of the terms we obtain

$$F_1 = \prod_{q=0,\, q\neq Q}^{\left\lfloor \frac{N-1}{2} \right\rfloor} \cos\left(\theta_q - \tilde{\theta}_q\right) \cdot \Big(\cos^2\theta_q \cos^2\tilde{\theta}_Q + \cos^2\theta_q \sin^2\tilde{\theta}_Q \tag{C.2}$$

$$+ \sin^2\theta_q \cos^2\tilde{\theta}_Q + \sin^2\theta_q \sin^2\tilde{\theta}_Q \Big) \tag{C.3}$$

$$= \prod_{q=0,\, q\neq Q}^{\left\lfloor \frac{N-1}{2} \right\rfloor} \cos\left(\theta_q - \tilde{\theta}_q\right). \tag{C.4}$$

It's worth noting that in the case of $Q = 0, \pi$ the whole bracket actually consists of only a $\cos\theta_q \cos\tilde{\theta}_Q = 1$, since instead of the whole expression for χ_Q we have a trivial relation $\chi_{0,\pi} = \psi_{0,\pi}$ and there is no rotation, and therefore no θ_q.

C.2 Natural variables

Since in region I of the phase diagram u^* is constant along parabolas of the form

$$h(\gamma) = C(1 - \gamma^2) \tag{C.5}$$

Then we can look for the bundle of the orthogonal curves to these parabolas. These will represent the direction over which the ground state changes.

We can start by noticing that the parabolas satisfy

$$\begin{aligned} y'(x) &= -2Cx \\ C &= -\frac{y'}{2x} \\ y'(x) &= -\frac{2x\, y(x)}{1-x^2} \end{aligned} \tag{C.6}$$

Therefore, the set of orthogonal curves will satisfy

$$\begin{aligned} \int \frac{1-x^2}{x}\, dx &= \int 2y\, dy \\ \log\, x - \frac{x^2}{2} &= y^2(x) + \delta \end{aligned} \tag{C.7}$$

Then our mapping would be defined by solving

$$y = C(1-x^2) \tag{C.8a}$$

$$y^2 + \frac{x^2}{2} + \delta = \log\, x \tag{C.8b}$$

However, it can be simpler to study the inverse mapping

$$C = \frac{h}{1-\gamma^2} \tag{C.9a}$$

$$\delta = -\frac{\gamma^2}{2} - h^2 + \log\gamma \tag{C.9b}$$

C.3 Global fidelity graphs

C.4 Fidelity susceptibility

First, we should notice that the integral goes over half the Brillouin zone. Luckily, the integrand is an even function, so we can easily expand the integral $\int_0^\pi = \frac{1}{2}\int_0^{2\pi}$. Then, by the standard substitution $z = e^{i\phi}$ we turn the integral into a complex integral.

$$I = -\frac{1}{16\pi}\int_0^{2\pi} dk \left\{ \frac{c(1+\gamma^2)+\cos k}{[c(1-\gamma^2)+\cos k]^2 + \gamma^2 \sin^2 k} \right\}^2 \sin^2 k \tag{C.10}$$

$$= -\frac{1}{16\pi i}\oint_{\mathcal{C}} \frac{dz}{z} \left\{ \frac{[2zc(1+\gamma^2)+z^2+1](z^2-1)}{[2zc(1-\gamma^2)+z^2+1]^2 - \gamma^2(z^2-1)^2} \right\}^2 \tag{C.11}$$

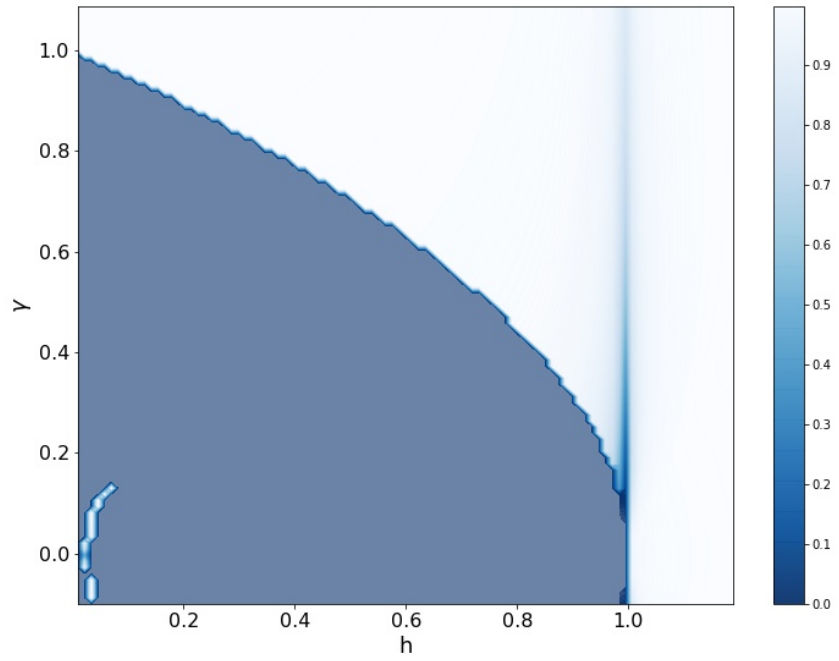

Figure C.1: Fidelity in the case of antiferromagnetic order $J = 1$ for $N = 507$. Already at $N = 507$ we can see the level crossings become essentially continuous.

The contour for this integral is a simple unit circle. The poles of this integral, which are found by looking for the points for which the denominator vanishes, are the following

$$z_1^{\pm} = \frac{-c(1-\gamma^2) + i\sqrt{(1-\gamma^2)[1-c^2(1-\gamma^2)]}}{1 \pm \gamma}, \tag{C.12a}$$

$$z_2^{\pm} = \overline{z}_1^{\pm}, \quad z_0 = 0. \tag{C.12b}$$

One can easily check, by keeping in mind we're considering region I that, along with z_0, the poles inside the unit circle are z_1^+ and $z_2^+ = \overline{z}_1^+$. Utilizing the residuum theorem we arrive at the solution

$$I = \frac{1}{16} \frac{1 + c^2(1+\gamma)^3(3\gamma - 1)}{\gamma(1+\gamma)^2(1 - c^2(1-\gamma^2)^2)}. \tag{C.13}$$

Appendix D Reduced fidelity

D.1 Operators A,B

Let us look at commutation relations of the newly defined operators A_i and B_i.

$$\{A_i, A_j\} = \{\psi_i^\dagger, \psi_j^\dagger\} + \{\psi_i^\dagger, \psi_j\} + \{\psi_i, \psi_j^\dagger\} + \{\psi_i, \psi_j\} \tag{D.1}$$

$$= 2\delta_{ij} \tag{D.2}$$

$$= \{A_i, A_j^\dagger\}. \tag{D.3}$$

Doing the same for B_i brings us

$$\{B_i, B_j\} = -2\delta_{ij}\{B_i, B_j^\dagger\}. \tag{D.4}$$

Finally, A_i and B_i anti-commute

$$\{A_i, B_j\} = 0. \tag{D.5}$$

The product of operators A_iB_i can be written over operators ψ_i in another way

$$A_iB_j = (\psi_i^\dagger + \psi_i)(\psi_i^\dagger - \psi_i) \tag{D.6}$$

$$= -\psi_i^\dagger\psi_i + \psi_i\psi_i^\dagger \qquad \text{(utilizing } (\psi_i)^2 = 0\text{)}$$

$$= 1 - 2\psi_i^\dagger\psi_i. \tag{D.7}$$

We can easily show the correlator $\langle A_iA_j\rangle$ vanishes

$$\langle A_iA_j\rangle = \langle(\psi_i^\dagger + \psi_i)(\psi_j^\dagger + \psi_j)\rangle = \langle\psi_i^\dagger\psi_j + \psi_i\psi_j^\dagger\rangle = \delta_{ij} = 0,$$

where we have used the commutation relations (2.8) and the fact that $i \neq j$ always. An analogous procedure proves also $\langle B_iB_j\rangle = 0$

D.2 Frustrated ground state

We can start with the following expectation

$$\begin{aligned}\langle\psi_k\psi_q\rangle &= \{k, q \neq \pi\} \\ &= \frac{1}{2}\Big[\,\langle GS^*|\,\chi_k^*\chi_\pi + \langle GS^*|\,\chi_{-k^*}\chi_\pi\Big]\Big(\cos\theta_k\chi_k - \sin\theta_k\chi_{-k}^\dagger\Big) \\ &\quad \Big(\cos\theta_q\chi_q - \sin\theta\chi_{-q}^\dagger\Big)\Big[\chi_\pi^\dagger\chi_{k*}^\dagger\,|GS^*\rangle + \chi_\pi^\dagger\chi_{-k^*}\,|GS^*\rangle\,\Big]\end{aligned} \tag{D.8}$$

We need to calculate different combinations of χ_q operators using their commutation relations 2.37. For example, we can start by

$$\begin{aligned}\chi_{k^*}\chi_\pi\chi_k\chi_{-q}^\dagger\chi_\pi^\dagger\chi_{k^*}^\dagger &= \chi_{k^*}\chi_\pi(\delta_{k,-q} - \chi_{-q}^\dagger\chi_k)\chi_\pi^\dagger\chi_{k^*}^\dagger \\ &= \chi_{k^*}\chi_\pi\chi_\pi^\dagger(\delta_{k,-q} - \chi_{-q}^\dagger\chi_k)\chi_{k^*}^\dagger \\ &= \chi_{k^*}(1-\chi_\pi\chi_\pi^\dagger)\delta_{k,-q}\chi_{k^*} - \chi_{k^*}\chi_\pi\chi_\pi^\dagger\chi_{-q}^\dagger(\delta_{k,k^*} - \chi_{k^*}^\dagger\chi_k) \\ &= \chi_{k^*}\delta_{k-q}\chi_{k^*}^\dagger - \chi_{k^*}(1-\chi_\pi\chi_\pi^\dagger)\delta_{k,k^*}\chi_{-q}^\dagger \\ &= \delta_{k,-q} - \delta_{k^*,-q}\delta_{k,k^*}\end{aligned} \tag{D.9}$$

Similarly we get the other 15 terms

$$\begin{aligned}&\chi_{k^*}\chi_\pi\chi_k\chi_{-q}^\dagger\chi_\pi^\dagger\chi_{-k^*}^\dagger = -\delta_{k^*,-q}\delta_{k,-k*}, && \chi_{\pm k^*}\chi_\pi\chi_{-k}^\dagger\chi_q\chi_\pi^\dagger\chi_{\pm k^*}^\dagger = \delta_{\pm k^*,-k}\delta_{k*,\pm q}, \\ &\chi_{-k^*}\chi_\pi\chi_k\chi_{-q}^\dagger\chi_\pi^\dagger\chi_{k^*}^\dagger = -\delta_{-k^*,-q}\delta_{k,k*}, && \chi_{-k^*}\chi_\pi\chi_k\chi_{-q}^\dagger\chi_\pi^\dagger\chi_{-k^*}^\dagger = \delta_{k,-q} - \delta_{-k^*,-q}\delta_{k,-k^*}, \\ &\chi_{\pm k^*}\chi_\pi\chi_k\chi_q\chi_\pi^\dagger\chi_{\pm k^*}^\dagger = 0, && \chi_{\pm k^*}\chi_\pi\chi_{-k}^\dagger\chi_{-q}^\dagger\chi_\pi^\dagger\chi_{\pm k^*}^\dagger = 0,\end{aligned} \tag{D.10}$$

$$\begin{aligned}\langle\psi_k\psi_q\rangle &= \frac{1}{2}\Big\{ - \cos\theta_k\sin\theta_q\big(\delta_{k,-q} - \delta_{k,k*}\delta_{k*,-q} - \delta_{k,-k*}\delta_{k*,-q} - \delta_{k,k^*}\delta_{-q,-k^*} + \delta_{k,-q} - \delta_{k,-k^*}\delta_{-q,-k^*}\big), \\ &\qquad - \sin\theta_k\cos\theta_q\big(\delta_{k^*,q}\delta_{-k,k^*} + \delta_{-k^*,q}\delta_{-k,k^*} + \delta_{k^*,q}\delta_{-k,-k^*} + \delta_{-k^*,q}\delta_{-k,-k^*}\big)\Big\}, \\ \langle\psi_k\psi_q\rangle &= \frac{1}{2}\delta_{k,-q}\cos\theta_q\sin\theta_q\big(1 - \delta_{q,-k^*} - \delta_{q,k^*}\big).\end{aligned} \tag{D.11}$$

The rest of the correlators are obtained analogously.

5 Prošireni sažetak

5.1 Uvod

"Cjelina je više od sume svojih dijelova". Navodna Aristotelova izreka često se koristi za opis sustava mnoštva čestica. Iako pronalazimo kompleksne sustave s različitim manifestacijama kompleksnosti u svim sferama života, pojam *sustavi mnoštva čestica* uglavnom se koristi u kontekstu fizikalnog sustava koji se sastoji od mnogo čestica te su njihove interakcije najčešće kvantne prirode. Pod pojam *mnoštvo* tehnički spadaju svi sustavi s više od 2 čestice, no sustavi od 3 i 4 čestice ipak čine posebnu kategoriju sa svojim metodama rješavanja. Glavna je problematika sustava mnoštva čestica ta što nije moguće riješiti sustav 10^{23} Schrödingerovih jednadžbi, čak i kada bismo ih mogli napisati. Stoga, pristup rješavanju ove kategorije problema često odudara od uobičajenog redukcionizma, tj. prikazu sustava kroz njegove konstituente. Jedan od istaknutih primjera "uobičajenog" pristupa je Landau-Ginzburg teorija koja opisuje čitave klase problema kroz jedan parametar uređenja koji potječe od relevantne simetrije sustava čiji lom uzrokuje fazni prijelaz. U toj teoriji, koja čini glavni pristup i klasičnim i kvantnim faznim prijelazima, intenzivne odrednice poput rubnih uvjeta odbacuju se kao nerelevantne za formiranje uređenja. No, posljednjih godina opažaju se slučajevi gdje specifični rubni uvjeti utječu i izazivaju promjene na sustavima. Ta vrsta rubnih uvjeta uzrokuje frustraciju te se zato naziva *frustrirani rubni uvjeti* (engl. FBC). FBC odgovaraju sustavu koji ima antiferomagnetsko uređenje, neparan broj "čestica" (npr. spinova) i periodične rubne uvjete. Periodični rubni uvjeti mogu se postići i spajanjem lanca u krug. Frustracija je širok pojam, no u svojoj srži ona potječe od nemogućnosti sustava da ispuni zadane uvjete te ju je najlakše objasniti kroz klasičnu geometrijsku frustraciju. Zamislimo kvadrat u čijim su vrhovima postavljena četiri spina kao u "kvadratni lanac". Spinovi interagiraju antiferomagnetski, što znači da se postavljaju antiparalelno. Nemamo nikakvih problema ispuniti taj uvjet već samo izaberemo orijentaciju početnog spina i ostale postavimo tako da ispunjavaju antiparalelnost. Kada bismo pokušali napraviti isto na primjeru trokuta, ubrzo bismo saznali kako nije moguće postaviti spinove bez da su barem dva paralelno postavljena – sustav je frustriran jer ne može ispuniti svoje antiferomagnetsko uređenje. Glavni cilj ovog rada proučiti je utjecaj frustracije na geometrijska svojstva osnovnog stanja kroz usporedbu frustriranog i nefrustriranog

sustava. Geometrija osnovog stanja opisana je kroz kvantni metrički tenzor. Kvantni metrički tenzor realni je i simetrični dio kompleksnog kvantnog geometrijskog tenzora. On mjeri udaljenost (tj. preklop) između dvaju stanja. Za ovu analizu izabran je jednodimenzionalni XY model u transverzalnom magnetskom polju, prototipični kvantno-mehanički spinski model. Sastoji se od interakcije susjednih spinova xx i yy komponenti čija se razlika opisuje parametrom anizotropije γ te interakcije s magnetskim poljem h u z smjeru.

$$H = \frac{J}{2}\sum_{j=1}^{N}\left(\frac{1+\gamma}{2}\sigma_j^x\sigma_{j+1}^x + \frac{1-\gamma}{2}\sigma_j^y\sigma_{j+1}^y\right) - \frac{h}{2}\sum_{j=1}^{N}\sigma_j^z. \tag{5.12}$$

Radi se o 1D rešetci s N mjesta na kojima se nalazi trodimenzionalni spin od $1/2$, a parametar J opisuje glavno uređenje sustava. Za $J < 0$ radi se o feromagnetskom, a za $J > 0$ antiferomagentskom uređenju. Ovaj model ima egzaktno analitičko rješenje, no netrivijalan fazni dijagram na apsolutnoj nuli temperatuer te je zato idealan za testiranje novih metoda. Za $\gamma = 0$ model postaje tzv. izotropni XX model, dok za $h = 1$ imamo Isingov model. Frustracija će dovesti do odvajanja posebne regije $h < 1 - \gamma^2$ koju će trebati posebno proučiti. Na apsolutnoj nuli temperature radi se o kvantnim faznim prijelazima. Kvantni fazni prijelazi uzrokovani su kvantnim fluktuacijama i podrazumijevaju (drastičnu) promjenu osnovnog stanja, no moguće ih je tretirati Landau-Ginzburg formalizmom. Kako bismo proučili utjecaj frustracije na geometriju osnovnog stanja koristit ćemo relativno novu metodu. Vjernost (engl. *fidelity*) je veličina klasično korištena u kvantnoj informaciji, no uvedena je u ovo područje kao potencijalno vrijedna metoda za proučavanje faznih prijelaza. Vjeruje se da je uz pomoć vjernosti moguće konstruirati fazni dijagram sustava bez ikakvih svojstava poznatih *a priori*. Vjernost je, u principu, funkcija preklopa dvaju stanja.

$$F(\Psi', \Psi) = |\,\langle\Psi'|\Psi\rangle\,|. \tag{5.13}$$

Ideja je da se pri sporom variranju parametara h i γ gleda vjernost između "susjednih“ stanja. U slučaju drastične promjene trebalo bi doći do naglog pada u vrijednosti vjernosti, efektivno signalizirajući postojanje faznog prijelaza. Također, moguće je definirati susceptibilnost vjernosti koja direktno odgovara već spomenutom kvatnom metričkom tenzoru. U slučaju kontinuiranih energetskih prijelaza (engl. *level-*

crossing) nije moguće definirati globalnu susceptibilnost već je potrebno otići korak dalje te izračunati reduciranu vjernost. Reducirana vjernost promatra podsustave umjesto cijelog sustava čime efektivno smanjuje "oštrinu“ ortogonalnosti te postaje moguće definirati i izračunati susceptibilnost.

U Poglavlju 2 detaljno rješavamo XY lanac standardnom proceduro, a zatim i proučavamo osnovno stanje sustava s obzirom na uređenje ($J = \pm 1$), paritet broja spinova te položaj u parametarskom prostoru. U sljedećem, Poglavlju 3 računamo vjernost za relevantna osnovna stanja sustava te diskutiramo razliku u rezultatima. Finalno, u Poglavlju 3.2 računamo korelacijske funkcije kako bismo izračunali reduciranu vjernost i njenu susceptibilnost.

5.2 Rješavanje XY lanca

Standardna procedura rješavanja XY lanca podrazumijeva Jordan-Wigner preslikavanje spinova u sustav fermiona kao prvi korak. Nakon toga slijedi dijeljenje hamiltonijana u dva sektora pomoću operatora pariteta. Tako podijeljeni hamiltonijani mogu se dovesti u dijagonalnu formu slobodnih fermiona.

Zapisivanjem hamiltonijana preko Paulijevih operatora dizanja i spuštanja

$$\sigma^{+,-} = \frac{1}{2}(\sigma^x \pm i\sigma^y), \tag{5.14}$$

dobivamo:

$$H = \frac{J}{2}\sum_{j=1}^{N}\left(\sigma_j^+\sigma_{j+1}^- + \gamma\sigma_j^+\sigma_{j+1}^+ + \text{h.c.}\right) - \sum_{j=1}^{N} h\sigma_j^z. \tag{5.15}$$

Ovaj hamiltonijan preslikava se u fermionski sustav pomoću Jordan-Wigner transformacije

$$\psi_j = \left(\prod_{l=1}^{j-1}\sigma_l^z\right)\sigma_j^+, \tag{5.16a}$$

$$\psi_j^\dagger = \left(\prod_{l=1}^{j-1}\sigma_l^z\right)\sigma_j^-. \tag{5.16b}$$

Ovi operatori zadovoljavaju fermionske relacije

$$\{\psi_i, \psi_j\} = 0, \tag{5.17a}$$

$$\{\psi_i, \psi_j^\dagger\} = \delta_{ij}. \tag{5.17b}$$

Uvođenjem operatora pariteta $[H, P] = 0$

$$P = \prod_{l=1}^{N} \sigma_l^z = \prod_{l=1}^{N} \left(1 - 2\psi_l^\dagger \psi_l\right), \tag{5.18}$$

slijedi podjela hamiltonijana na sektore prema svojstvenim vrijednostima operatora pariteta ± 1.

$$H = \frac{1+P}{2} H^+ \frac{1+P}{2} + \frac{1-P}{2} H^- \frac{1-P}{2}, \tag{5.19}$$

uz

$$\begin{aligned} H^\pm = &- \frac{J}{2} \sum_{j=1}^{N-1} \left(\psi_j \psi_{j+1}^\dagger + \gamma \psi_j \psi_{j+1} + \text{ h.c. }\right) \pm \frac{J}{2} \left(\psi_N \psi_1^\dagger + \gamma \psi_N \psi_1 + \text{ h.c. }\right) \\ &+ h \sum_{j=1}^{N} \psi_j^\dagger \psi_j - \frac{1}{2} N h. \end{aligned} \tag{5.20}$$

Nakon prelaska u Fourierov prostor te Bogoljubove rotacije dolazimo do hamiltonijana slobodnih fermiona

$$H^\pm = \sum_q \Lambda_q \left(\chi_q^\dagger \chi_q - \frac{1}{2}\right), \tag{5.21}$$

gdje su χ_q fermionski operatori u Fourierovom prostoru. Skup q po kojem se sumira ovisi o sektoru. $q \in X_N$, $X_N = \{x_0, x_0 + 1, x_0 + 2, ..., x_0 + N - 1\}$, gdje je $x_0 = 1/2$ u parnom i $x_0 = 0$ u neparnom sektoru.

Spektar je dan sa sljedećim izrazom

$$\Lambda_q \equiv \Lambda\left(\frac{2\pi}{N} q\right) \equiv \sqrt{\left[h + J\cos\left(\frac{2\pi}{N} q\right)\right]^2 + J^2\gamma^2 \sin^2\left(\frac{2\pi}{N} q\right)}. \tag{5.22}$$

Treba uzeti u obzir da za specijalne momente $k = 0, \pi$ energija nije definirana preko navedene funkcije lambde nego je dana s $h \pm 1$, što omogućuje negativne doprinose sumi te, posljedično, frustraciju.

U slučaju feromagentskog uređenja imamo jednostavno vakuum kao osnovo stanje sustava u parnom sektoru, a u neparnom se sektoru dodaje ekscitacija $q = 0$ kako bi se dobio potreban paritet. U termodinamičkom limitu ova dva sektora postaju degenerirana.

$$|GS^+\rangle = \prod_{q=0}^{\left\lfloor \frac{N}{2} \right\rfloor - 1} \left(\cos\theta_{q+1/2} + \sin\theta_{q+1/2}\, \psi^\dagger_{q+1/2} \psi^\dagger_{-(q+1/2)} \right) |0\rangle = |vac\rangle\,, \tag{5.23}$$

$$|GS^-\rangle = \chi_0^\dagger\, |vac\rangle\,. \tag{5.24}$$

U antiferomagnetskom uređenju za paran N imamo identičnu situaciju kao u feromagnetskom slučaju samo s pobuđenjem $k = \pi$ umjesto $k = 0$. Za neparan N dolazimo do zanimljivih pojava. Parametarski prostor se dijeli na 3 dijela u parnom sektoru: $h > 1$, dok se $h < 1$ dijeli na $h >, < 1 - \gamma^2$. U području $h < 1 - \gamma^2$ pojavljuju se specijalne točke simetričnih minimuma $\pm k^* = \arccos \frac{h}{1-\gamma^2}$ koje omogućuju da u parnom sektoru dodamo negativni π mod.

$$|GS^+, h > 1 - \gamma^2\rangle = |vac\rangle\,, \tag{5.25}$$

$$|GS^+, h < 1 - \gamma^2\rangle = \chi^\dagger_\pi \left(\chi^\dagger_{k^*} + \chi^\dagger_{-k^*} \right) |vac\rangle\,. \tag{5.26}$$

To je direktna posljedica frustracije. Također, ispostavlja se da u području $1 - \gamma^2 < h < 1$, unatoč vakuumu kao osnovnom stanju dolazi do frustracije sustava, što je vidljivo u energiji.

$$E_{h>1} = -\frac{1}{2} \sum_{q=0}^{N-1} \Lambda_{q+\frac{1}{2}}, \tag{5.27}$$

$$E_{1-\gamma^2<h<1} = -\frac{1}{2} \sum_{q=0}^{N-1} \Lambda_{q+\frac{1}{2}} + \Lambda_\pi, \tag{5.28}$$

$$E_{h<1-\gamma^2} = -\frac{1}{2} \sum_{q=0}^{N-1} \Lambda_{q+\frac{1}{2}} + \Lambda_*. \tag{5.29}$$

5.3 Globalna vjernost

Koristimo vjernost i pripadnu susceptibilnost kako bismo odredili geometrijska svojstva osnovnog stanja sustava. Kako variramo parametre h i γ, očekujemo snažan pad pri računanju vjernosti u blizini kritičnih točaka. Izveli smo izraz za vjernost sve

tri neiščezavajuće kombinacije osnovnih stanja (preklop različitih stanja odmah daje egazktnu nulu budući da su ortogonalna).

$$\mathcal{F}_t = \prod_{q=0, q\neq Q_t}^{\left\lfloor \frac{N-1}{2} \right\rfloor} \cos\left(\theta_q - \tilde{\theta}_q\right). \tag{5.30}$$

Sve tri kombinacije su dale isti izraz do na člana umnoška s momentom Q. Indeks t označava o kojem osnovnom stanju se radi, dok je Q_t pripadajući moment kojeg izbacujemo iz umnoška. $Q_0 = 0,\ Q_1 = 0, \pi,\ Q_2 = k^*$.

Susceptibilnost se može izvesti razvijanjem vjernosti u red po parametrima h i γ

$$g_{i,j} = -\sum_{q'} \partial_i \theta_{q'}\, \partial_j \theta_{q'}. \tag{5.31}$$

U nefrustriranom slučaju elementi kvantnog matričnog tenzora su

$$g_{hh} = \frac{1}{16} \begin{cases} \frac{1}{|\gamma|(1-h^2)}, & |h| < 1 \\ \frac{|h|\gamma^2}{(h^2-1)(h^2-1+\gamma^2)^{3/2}}, & |h| > 1 \end{cases} \tag{5.32a}$$

$$g_{\gamma\gamma} = \frac{1}{16} \begin{cases} \frac{1}{|\gamma|(1+|\gamma|)^2}, & |h| < 1 \\ \left[\frac{2}{(1-\gamma^2)^2}\left(\frac{|h|}{\sqrt{h^2-1+\gamma^2}} - 1\right) - \frac{|h|\gamma^2}{(1-\gamma^2)(h^2-1+\gamma^2)^{3/2}}\right], & |h| > 1 \end{cases} \tag{5.32b}$$

$$g_{h\gamma} = \frac{1}{16} \begin{cases} 0, & |h| < 1 \\ \frac{-|h|\gamma}{h(h^2-1+\gamma^2)^{3/2}}, & |h| > 1 \end{cases} \tag{5.32c}$$

U feromagnetskom slučaju jasno vidimo snažan pad u vjernosti za očekivane fazne prijelaze $h = 1$ i $\gamma = 0$. S druge strane, pri antiferomagnetskom slučaju uz neparan N, uz poznate fazne prijelaze vidimo još velik broj diskontinuiteta gdje vjernost pada egzaktno na nulu. Ti prijelazi odgovaraju promjeni k^* s promjenom parametara. Budući da je vjernost identički nula u tim točkama, nije moguće definirati susceptibilnost osim duž svake parabole $h = c(1-\gamma^2)$ koja drži k^* konstantnim.

$$\tilde{g}_{\gamma\gamma} = -\frac{1}{16}\frac{1 + c^2(1+\gamma)^3(3\gamma-1)}{\gamma[1+\gamma)^2(1-c^2(1-\gamma^2)^2]} + \frac{1}{4N}\frac{c^2(1-c^2)}{[1-c^2(1-\gamma^2)]^2}. \tag{5.33}$$

5.4 Reducirana vjernost

Zbog nemogućnosti provedbe daljnje analize uzrokovane pojavom mnoštva energetskih prijelaza (koji bi u termodinamičkom limitu prešli u kontinuirane), prelazimo na račun reducirane vjernosti

$$\mathcal{F}^R = \mathrm{Tr}\,\sqrt{\rho^{1/2}\tilde{\rho}\rho^{1/2}}, \tag{5.34}$$

gdje ρ označava reduciranu matricu osnovnog stanja (h, γ), a $\tilde{\rho} = \rho(h + dh, \gamma + d\gamma)$ reduciranu matricu sustava s bliskim parametrima. Budući da ideja reducirane vjernosti počiva na reduciranim matricama gustoće sustava, potrebne su nam korelacijske funkcije. Odabrali smo promatrati korelatore dvaju spinova.

$$\rho_{ij} = \sum_{\alpha,\beta=0}^{3} \langle \sigma_i^\alpha \sigma_j^\beta \rangle \; \sigma_i^\alpha \otimes \sigma_j^\beta. \tag{5.35}$$

Korelacijske funkcije smo računali na način da smo morali ponovno prolaziti kroz transformacije već napravljene za rješavanje sustava, kako bismo došli do korelatora čije vrijednosti znamo. Raspisujući gornje spomenutu definiciju matrice gustoće u bazi $\{|\uparrow\uparrow\rangle, |\uparrow\downarrow\rangle, |\downarrow\uparrow\rangle, |\downarrow\downarrow\rangle\}$,dobivamo sljedeći izraz

$$\rho_{ij} = \frac{1}{4}\begin{pmatrix} a^+ & 0 & 0 & c^- \\ 0 & b & c^+ & 0 \\ 0 & c^+ & b & 0 \\ c^- & 0 & 0 & a^- \end{pmatrix}, \tag{5.36}$$

s

$$a^\pm = 1 \pm \langle \sigma_i^z \rangle \pm \langle \sigma_j^z \rangle + \langle \sigma_i^z \sigma_j^z \rangle, \tag{5.37a}$$

$$b = 1 - \langle \sigma_i^z \sigma_j^z \rangle, \tag{5.37b}$$

$$c^\pm = \langle \sigma_i^x \sigma_j^x \rangle \pm \langle \sigma_i^y \sigma_j^y \rangle. \tag{5.37c}$$

Sljedeći korak prelazak je u Jordan-Wigner fermione

$$\langle \sigma_i^x \sigma_j^x \rangle = \Big\langle \prod_{l=j}^{i-1} (1 - 2\psi_l^\dagger \psi_l)(\psi_i + \psi_i^\dagger)(\psi_j + \psi_j^\dagger) \Big\rangle. \tag{5.38}$$

Sada uvodimo nove operatore A_i i B_i

$$A_i \equiv \psi_i^\dagger + \psi_i, \quad B_i \equiv \psi_i^\dagger - \psi_i. \tag{5.39}$$

Novodefinirani operatori omogućuju nam da $\langle \sigma_i^\alpha \sigma_j^\alpha \rangle$ zapišemo kao očekivanje umnoška takve forme koja nam nakon korištenja Wickovog teorema daje sljedeće izraze

$$\langle \sigma_i^x \sigma_j^x \rangle = \sum_p (-1)^p \big\langle B_j A_{P(j+1)} \big\rangle \big\langle B_{j+1} A_{P(j+2)} \big\rangle \cdot \cdots \cdot \big\langle B_{i-1} A_{P(i)} \big\rangle, \tag{5.40a}$$

$$\langle \sigma_i^y \sigma_j^y \rangle = \sum_p (-1)^p \big\langle B_{j+1} A_{P(j)} \big\rangle \big\langle B_{j+2} A_{P(j+1)} \big\rangle \cdot \cdots \cdot \big\langle B_i A_{P(i-1)} \big\rangle, \tag{5.40b}$$

$$\langle \sigma_i^z \sigma_j^z \rangle = \big\langle B_i A_i \big\rangle \big\langle B_j A_j \big\rangle - \big\langle B_i A_j \big\rangle \big\langle B_i A_j \big\rangle. \tag{5.40c}$$

Prethodni izrazi mogu se prepoznati kao zapis determinante matrice.

Preostaje račun elemenata matrice kroz ponovno korištenje već dobro poznatih transformacija. Treba imati na umu da će račun koji slijedi ovisiti s kojim osnovnim stanjem radimo. Dosadašnji raspis bio je generalan.

Traženi elementi matrice za vakuumsko su osnovno stanje sljedeći

$$\big\langle A_i B_i \big\rangle = \langle 1 - 2\psi_i^\dagger \psi_i \rangle = 1 - \frac{2}{N} \sum_q \sin^2 \theta_q, \tag{5.41a}$$

$$\begin{aligned} \big\langle A_i B_j \big\rangle &= \langle (\psi_i^\dagger + \psi_i)(\psi_j^\dagger - \psi_j) \rangle \\ &= -\frac{1}{N} \sum_q \left\{ \sin 2\theta_q \sin \left[\frac{2\pi}{N} q(i-j) \right] + \cos 2\theta_q \cos \left[\frac{2\pi}{N} q(i-j) \right] \right\}, \end{aligned} \tag{5.41b}$$

$$\big\langle B_i A_j \big\rangle = -\big\langle A_j B_i \big\rangle = \frac{1}{N} \sum_q \left\{ -\sin 2\theta_q \sin \left[\frac{2\pi}{N} q(i-j) \right] + \cos 2\theta_q \cos \left[\frac{2\pi}{N} q(i-j) \right] \right\}. \tag{5.41c}$$

U regijama gdje postoji frustracija uz vakuumski doprinos dobiva se i član korekcije. Finalne verzije korelatora su:

$$\big\langle A_i B_j \big\rangle = \big\langle A_i B_j \big\rangle_0 + C^{(1)} + C^{(2)}(h, \gamma), \tag{5.42}$$

gdje je s indeksom 0 označen temeljni vakuumski doprinos.

$$C^{(1)} = \begin{cases} -\frac{2}{N}\cos\left[\frac{2\pi}{N}q(i-j)\right], & h<1 \\ 0, h>1 \end{cases} \tag{5.43}$$

$$C^{(2)}(h,\gamma) = \begin{cases} \frac{2}{N}\left(\cos\frac{4\pi}{N}k^*i - \cos 2\theta_*\right), & i=j,\ h<1-\gamma^2 \\ \frac{2}{N}\left[\sin 2\theta_* \sin(i-j)k^* - \cos 2\theta_* \cos(i-j)k^* + \cos(i+j)k^*\right], & i\neq j,\ h<1-\gamma^2 \\ 0, & h>1-\gamma^2 \end{cases} \tag{5.44}$$

Nakon finaliziranih reduciranih matrica gustoće, gledali smo ponašanje reducirane vjernosti kako variramo magnetsko polje h. Više ne primjećujemo diskontinuitete kao u globalnoj vjernosti, što znači da je reducirana vjernost uspješna barem u tom aspektu. No, vidimo drugo zanimljivo ponašanje. Za najnižu vrijednost N vidimo postojanje padova čije amplitude osciliraju. Ta oscilacija dolazi od korekcije na korelacijske funkcije uzrokovane frustracijom, koja sadrži članove koji osciliraju. Korekcija pada s $1/N$ što je, kao što vidimo, dovoljno brzo da već na sljedećem redu veličine oscilacije potpuno iščeznu. Na samom kraju postoji jedan više puta veći pad od oscilirajućih, koji opstaje i za veće N-ove. Taj pad odgovara posljednjoj paraboli $h = 1-\gamma^2$. Budući da je tako dominantan te da se nalazi na samoj granici specijalne regije parametarskog prostora, željeli smo provjeriti kako se amplituda tog pada ponaša s daljnjim rastom broja spinova. No, i u slučaju najbližih susjeda, i u slučaju ekstenzivne udaljenosti $\frac{N-1}{2}$, amplituda tzv. π-vrha opada s otprilike $1/N^2$, te to čini prilično pravilno.

5.5 Zaključak

Cilj ovog diplomskog rada bio je proučiti efekte frustracije na geometrijska svojstva osnovnog stanja kroz usporedbu frustriranog i nefrustriranog spinskog lanca. Kao model sustav izabran je XY lanac.

Na početku je predstavljen 1D XY model te je riješen analitički koristeći poznatu proceduru preslikavanja spinskog sustava u fermionski (Jordan-Wigner), zatim prelaska u Fourier prostor te Bogoljubov rotacije koja dovodi do konačnog dijagonalnog hamiltonijana. Analiza osnovnog stanja provedena je na vrlo detaljan način, uzimajući u obzir oba magnetska uređenja, parnost broja spinova, parnost sektora te poziciju kombinacije (h, γ) u parametarskom prostoru u odnosu na primijećene regije koje krase različita svojstva. Pomno su proučeni efekti izazvani frustracijom te je otkriveno da u slučaju antiferomagnetskog uređenja i neparnog broja spinova cijela regija $h < 1$ u parnom sektoru postaje frustrirana, očitujući se kroz (efektivne) ekscitacije u osnovnom stanju. Posebno je zanimljiva regija $h < 1 - \gamma^2$ gdje moment jedne od ekscitacija ovisi o parametrima h i γ, time se mijenjajući kroz parametarski prostor te izazivajući sve veći broj prijelaza energetskih razina s rastom broja spinova N. U termodinamičkom limitu, ti prijelazi postaju kontinuirani.

Nakon postavljanja samog modela, vraćamo se cilju rada koji je analiza geometrije osnovnog stanja kroz računanje vjernosti i pripadajuće susceptibilnosti između osnovnih stanja s blago različitim parametrima h i γ. Pretpostavlja se da bi vjernost trebala omogućiti konstrukciju faznog dijagrama danog sustava bez ikakvog *a priori* znanja o sustavu. Naime, vjernost, kao funkcija preklopa dvaju stanja, bi trebala pokazati nagli i izraziti pad pri dolasku do kritične točke. Napravljen je izračun preklopa stanja za sve neiščezavajuće kombinacije stanja (preklop različitih stanja automatski daje nulu) te je dobiven izraz jednak do na moment koji je isključen iz umnoška. Taj izraz je uspio generirati sve očekivano ponašanje. Uz poznate prijelaze $h = 1$, i $\gamma = 0$, vjernost je pokazala vrhove egzaktnog diskontinuiteta u frustriranoj regiji, koji su posljedica već spomenutih prijelaza energetskih razina. Iako je susceptibilnost vjernosti određena za ne-frustrirane regije, vjernost koje je gotovo kontinuirano identički nula onemogućuje nastavak analize. Napravljena je jedino susceptibilnost uzduž parabole, što je dodatno potvrdilo izvor tih diskontinuiteta.

Kako bi se ipak analizirala geometrijska svojstva te regije, uvedena je nova veličina koja se inače koristi za kontinuirane prijelaze, bazirana na proučavanju podsustava

umjesto čitavih sustava - radi se o reduciranoj vjernosti. Reducirana vjernost se temelji na korištenju reduciranih matrica gustoće, što je zahtijevalo određivanje korelacijskih funkcija dvostrukog spina (za različite regije). Ono što smo otkrili promatrajući reduciranu vjernost i pripadajuću susceptibilnost, jest da ti diskontinuiteti, koji bi po dosadašnjim pretpostavkama automatski trebali signalizirati fazni prijelaz, zapravo nestaju u termodinamičkom limitu. Našli smo protuprimjer općeprihvaćenoj pretpostavci da se analiza sustava kroz vjernost može koristiti za kompletnu izgradnju bez ikakvog *a priori* znanja o sustavu.

5.6 Nazivi slika i tablica na hrvatskom jeziku

Bibliography

[1] Landau, L. D. On the theory of phase transitions. // Zh. Eksp. Teor. Fiz. Vol. 7 (1937), 19–32.

[2] Sachdev, S. Quantum Phase Transitions. 2nd ed. Cambridge University Press, 2011.

[3] Shannon, N.; Momoi, T.; Sindzingre, P. Nematic order in square lattice frustrated ferromagnets. // Phys. Rev. Lett. Vol. 96 (2006), 027213.

[4] Marić, V.; Giampaolo, S. M.; Franchini, F. Quantum phase transition induced by topological frustration. // Communications Physics. Vol. 3, 1.

[5] Marić, V.; Giampaolo, S. M.; Kuić, D. et al. The frustration of being odd: how boundary conditions can destroy local order. // New Journal of Physics. Vol. 22, 8 (2020), 083024.

[6] Giampaolo, S. M.; Ramos, F. B.; Franchini, F. The frustration of being odd: universal area law violation in local systems. // Journal of Physics Communications. Vol. 3, 8 (2019), 081001.

[7] Campostrini, M.; Pelissetto, A.; Vicari, E. Quantum transitions driven by one-bond defects in quantum ising rings. // Phys. Rev. E. Vol. 91 (2015), 042123.

[8] Cheng, R. Quantum geometric tensor (fubini-study metric) in simple quantum system: A pedagogical introduction. // arXiv:1012.1337 (21/03/2021).

[9] Kolodrubetz, M.; Gritsev, V.; Polkovnikov, A. Classifying and measuring geometry of a quantum ground state manifold. // Physical Review B. Vol. 88, 6.

[10] Zanardi, P.; Paunković, N. Ground state overlap and quantum phase transitions. // Physical Review E. Vol. 74, 3.

[11] Rossini, D.; Vicari, E. Ground-state fidelity at first-order quantum transitions. // Physical Review E. Vol. 98, 6.

[12] Zhou, H.-Q.; Orús, R.; Vidal, G. Ground state fidelity from tensor network representations. // Physical Review Letters. Vol. 100, 8.

[13] GU, S.-J. Fidelity approach to quantum phase transitions. // International Journal of Modern Physics B. Vol. 24, 23 (2010), 4371–4458.

[14] Zanardi, P.; Giorda, P.; Cozzini, M. Information-theoretic differential geometry of quantum phase transitions. // Physical Review Letters. Vol. 99, 10.

[15] Zanardi, P.; Cozzini, M.; Giorda, P. Ground state fidelity and quantum phase transitions in free fermi systems. // Journal of Statistical Mechanics: Theory and Experiment. Vol. 2007, 02 (2007), L02002–L02002.

[16] Garnerone, S.; Jacobson, N. T.; Haas, S. et al. Fidelity approach to the disordered QuantumXYModel. // Physical Review Letters. Vol. 102, 5.

[17] Paunković, N.; Sacramento, P. D.; Nogueira, P. et al. Fidelity between partial states as a signature of quantum phase transitions. // Phys. Rev. A. Vol. 77 (2008), 052302.

[18] Kwok, H.-M.; Ho, C.-S.; Gu, S.-J. Partial-state fidelity and quantum phase transitions induced by continuous level crossing. // Physical Review A. Vol. 78, 6.

[19] Lieb, E.; Schultz, T.; Mattis, D. Two soluble models of an antiferromagnetic chain. // Annals of Physics. Vol. 16 (1961), 407–466.

[20] Katsura, S. Statistical mechanics of the anisotropic linear heisenberg model. // Physical Review. Vol. 127, 5 (1962), 1508–1518.

[21] Niemeijer, T. Some exact calculations on a chain of spins. // Physica. Vol. 36, 3 (1967), 377–419.

[22] Nielsen, M. A.; Chuang, I. L. Quantum computation and quantum information. Cambridge University Press, 2010.

[23] Osborne, T. J.; Nielsen, M. A. Entanglement in a simple quantum phase transition. // Physical Review A. Vol. 66, 3.

[24] Lieb, E.; Mattis, D. Mathematical Physics in One Dimension: Exactly Soluble Models of Interacting Particles. Perspectives in physics Academic Press, 1966.